

PAPER

[View Article Online](#)
[View Journal](#) | [View Issue](#)Cite this: *Dalton Trans.*, 2025, **54**, 9949

Manganese germylene complexes: reactivity with dihydrogen, isonitriles, and dinitrogen†

Jeffrey S. Price and David J. H. Emslie *

The manganese germylene-hydride complexes $[(\text{dmpe})_2\text{MnH}(\text{=GeR}_2)]$ (**1a**: R = Ph, **1b**: R = Et) reacted with H_2 (approx. 1.5 atm) to afford the 'germyl dihydride' species $[(\text{dmpe})_2\text{MnH}_2(\text{GeHR}_2)]$ (**2a**: R = Ph, **2b**: R = Et) as an equilibrium mixture with the starting material (**1a–b**). In solution, **2a–b** exist as a mixture of isomers where the major isomer (71–84%) is a *trans* hydrogermane hydride complex *trans*- $[(\text{dmpe})_2\text{MnH}(\text{GeHR}_2)]$ (**transHGe–2a–b**). The minor isomer of **2a–b** is tentatively assigned as the *cis* germyl dihydrogen complex *cis*- $[(\text{dmpe})_2\text{Mn}(\text{GeHR}_2)(\text{H}_2)]$ (**cis–2a–b**), possibly in rapid equilibrium with a small amount of the germanate complex $[(\text{dmpe})_2\text{Mn}(\text{H}_2\text{GeHR}_2)]$ (**central–2a–b**). DFT calculations were employed to gain insight into the nature of bonding in the isomers of **2a–b**, and an X-ray crystal structure was obtained for *trans*- $[(\text{dmpe})_2\text{MnH}(\text{HGeHEt}_2)]$ (**transHGe–2b**) which co-crystallized with **1b**. Reactions of **1a–b** with D_2 suggest a pathway that proceeds via conversion of **1a–b** to a 5-coordinate germyl intermediate $[(\text{dmpe})_2\text{Mn}(\text{GeHR}_2)]$ (**A**) prior to reaction with H_2/D_2 . Providing support for this pathway, intermediate **A** (R = Ph) was trapped via reactions of **1a** with isonitriles, affording the manganese(I) germyl isonitrile complexes $[(\text{dmpe})_2\text{Mn}(\text{GeHPh}_2)(\text{CNR})]$ (**3a**: R = ^tBu, **3b**: R = *o*-xylyl, and **3c**: R = ⁿBu). These complexes formed as a mixture of *cis* and *trans* isomers, and X-ray quality crystals were obtained for **cis–3a**, **cis–3b** and **trans–3c**. Complexes **1a–b** also reacted slowly with dinitrogen at room temperature to afford germyl dinitrogen complexes $[(\text{dmpe})_2\text{Mn}(\text{GeHR}_2)(\text{N}_2)]$ (**5a**: R = Ph, **5b**: R = Et). Compounds **5a–b** were initially formed as *cis* isomers, but the *trans* isomer is the thermodynamic product in each case, and the *cis* and *trans* isomers were crystallographically characterized for both **5a** and **5b**. X-ray crystallography, IR spectroscopy, and DFT calculations were employed to compare metal–dinitrogen bonding in the *cis* and *trans* isomers of **5a–b**. The silyl dinitrogen derivative $[(\text{dmpe})_2\text{Mn}(\text{SiHPh}_2)(\text{N}_2)]$ (**6**) was also generated as a mixture of the *cis* and *trans* isomers, and the *trans* isomer was structurally characterized. The *trans* isomers of **5b** and **6** show ⁵⁵Mn–³¹P coupling in the ³¹P{¹H} and ⁵⁵Mn{¹H} NMR spectra, affording 1 : 1 : 1 : 1 : 1 sextets and 1 : 4 : 6 : 4 : 1 quintets, respectively.

Received 1st May 2025,
Accepted 2nd June 2025

DOI: 10.1039/d5dt01025j

rsc.li/dalton

Introduction

Germylene (:GeR_2) ligands in transition metal complexes can serve as highly reactive sites, including for small molecule activation.^{1–4} Examples of reactivity involving germylene ligands include coordination of nucleophiles to germanium,^{5–8} Lewis base (RCN or pyridine) addition to a germylene hydride complex to afford a germyl complex,⁹ and migration of a hydrogen substituent in a GeHR ligand to the metal center to form a metallogermylene ($\text{L}_x\text{HM–GeR}$).^{10,11} Germylene to germylene transformations have also been demonstrated by

α -chloride migration,¹² loss of a hydride ligand and an alkyl substituent on germanium (as HR , where $\text{R} = \text{CH}_2\text{PMe}_2$),¹³ or dehydrogenation of an $[\text{L}_x\text{MH}(\text{=GeHR})]$ complex by reaction with an NHC, isocyanate or nitrile.^{7,8,14} Additionally, various reactions of $[\text{L}_x\text{MH}(\text{=GeHR})]^{x+}$ complexes with unsaturated substrates have been reported. For example, cationic complexes reacted with alkenes and alkynes to form hydrogermylation products,¹⁵ and neutral complexes reacted with aldehydes and ketones ($\text{R}'_2\text{C=O}$) to afford $[\text{L}_x\text{MH}(\text{=Ge}(\text{OCHR}'_2)\text{R})]$ (the latter reactions were proposed to proceed by $\text{R}'_2\text{C=O}$ coordination to Ge, nucleophilic attack at the carbonyl carbon by the metal hydride to form a germyl intermediate, and subsequent 1,1-deinsertion).^{5,9} Furthermore, $[\text{L}_x\text{MH}(\text{=GeHR})]$ complexes reacted with isocyanates or isothiocyanates to afford metallacyclic products containing a 5-membered MGeECN ($\text{E} = \text{O}$ or S) or MGeNCS ring.^{8,9,16} Addition of H_2O , MeOH , or NH_3 across a germylene M=Ge bond has also been reported, affording germyl hydride complexes with an OH, OMe or NH_2 substituent.

Department of Chemistry, McMaster University, 1280 Main St West, Hamilton, Ontario, L8S 4M1, Canada. E-mail: emslied@mcmaster.ca

†Electronic supplementary information (ESI) available: Overview of literature Mn(I) dinitrogen chemistry, selected NMR and IR spectra, SCD and PXRD data, and DFT results. CCDC 2447494–2447503. For ESI and crystallographic data in CIF or other electronic format see DOI: <https://doi.org/10.1039/d5dt01025j>

ent on germanium,^{17,18} and 2 + 2 cycloaddition has been observed or proposed in reactions of germylene complexes with CO₂ and isothiocyanates.^{9,19} Such reactivity offers many avenues for Ge incorporation into larger molecules. However, compared to lighter silylene^{2,20–23} and (especially) carbene^{24–26} complexes, the reactivity of transition metal germylene species is far less explored.

Recently, our group isolated the first terminal base-free germylene complexes of manganese, [(dmpe)₂MnH(=GeR₂)] (**1a**: R = Ph, **1b**: R = Et), by hydrogermane addition to Girolami and Wilkinson's^{27,28} manganese hydride complex [(dmpe)₂MnH(C₂H₄)] (top of Scheme 1),²⁹ which serves as a source of [(dmpe)₂MnEt].³⁰ While **1a–b** did not react with additional equivalents of H₂GeR₂, the monosubstituted derivative [(dmpe)₂MnH(=GeHⁿBu)] (**1c**) reacted with excess H₃GeⁿBu to produce a solution containing **1c** and H₃GeⁿBu in equilibrium with the products of hydrogermane addition; *trans*-[(dmpe)₂Mn(GeH₂ⁿBu)(HGeH₂ⁿBu)] and *mer*-[(dmpe)₂MnH(GeH₂ⁿBu)₂] (bottom of Scheme 1).²⁹ This reactivity suggests that the germylene-hydride complex **1c** exists in equilibrium with an undetected 5-coordinate manganese(i) germyl complex [(dmpe)₂Mn(GeH₂ⁿBu)] which is responsible for the observed reactivity with hydrogermanes.

We have previously reported the manganese silylene complexes [(dmpe)₂MnH(=SiR₂)]³¹ which are lighter congeners of **1a–b**, and their diverse (and in some cases highly unusual) reactivity with small molecules including H₂, H₂SiR₂, C₂H₄, CO₂, and C(NⁱPr)₂.^{31–34} Herein, we report reactions of the germylene-hydride complexes [(dmpe)₂MnH(=GeR₂)] (**1a–b**) with dihydrogen, isonitriles, and dinitrogen. Literature examples of reactivity of metal germylene complexes with these small molecules are scarce, though reactions with dihydrogen to form germyl hydride complexes have been reported for [(Et₃P)₂Pt(=Ge{N(SiMe₃)₂})₂],¹⁹ the heterobimetallic complex [(OC)Rh(μ-H)(μ-dppm)₂(μ-GePh₂)Ir(CO)](CF₃SO₃),³⁵ [(Cy₃P)₂RuH₂(H₂=GePh₂)] (in this case affording a mixture of germyl hydride and hydrogermane complexes),³⁶ [(Dipp²ArMe₂P)Pt(=GeCl

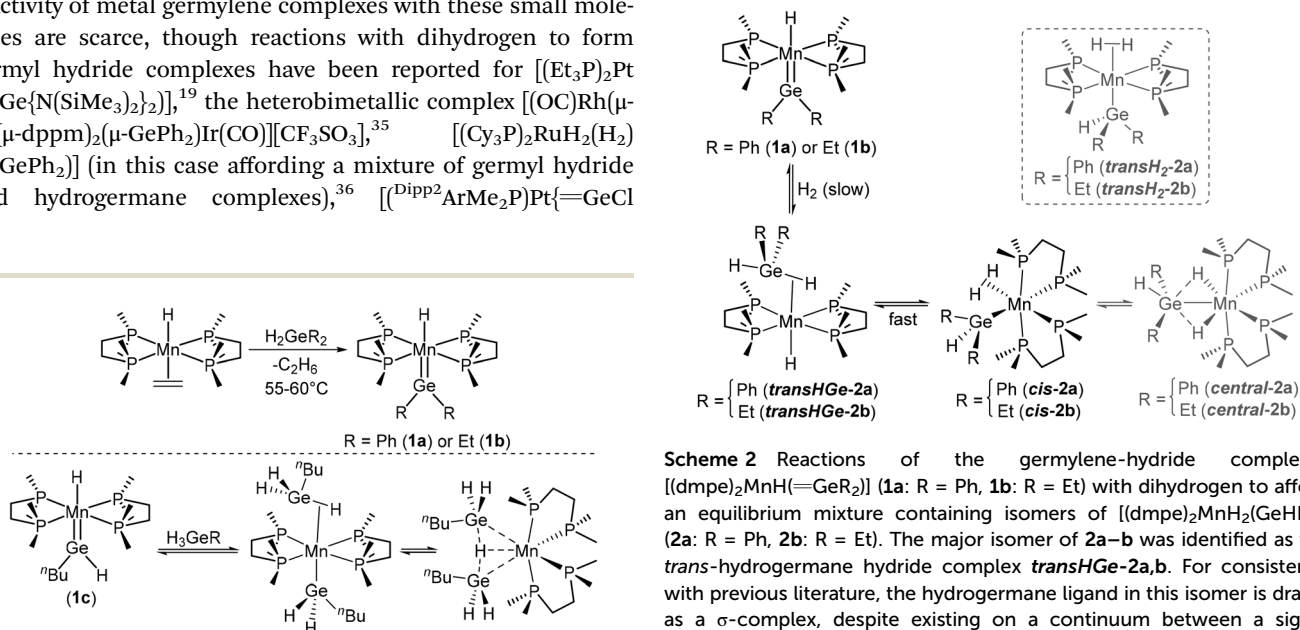
(Dipp²Ar))],¹⁸ and [(IPr)Ni(κ²-P,Ge-Ph₂PCH₂SiⁱPr₂N(Dipp)GeAr)].³⁷ A reaction of the titanium germylene complex [(THF)TiCp₂{=GeSi(SiMe^tBu)₂Si(SiMe^tBu)₂Si(SiMe^tBu)₂}] with an isonitrile has also been reported, but simply resulted in substitution of the THF co-ligand.³⁸

Results and discussion

Reactions with H₂

Solutions of the manganese germylene-hydride complexes *trans*-[(dmpe)₂MnH(=GeR₂)] (**1a**: R = Ph, **1b**: R = Et)²⁹ reacted with H₂ (~1.5 atm) at room temperature to afford the 'germyl dihydride' complexes [(dmpe)₂MnH₂(GeHR₂)] (**2a**: R = Ph, **2b**: R = Et); Scheme 2. These reactions only progressed to 87% (**2a**) or 73% (**2b**) conversion, reaching equilibrium with **1a–b** and H₂ within 3 days. This reactivity contrasts that of the silicon analogues which proceeded to completion (within a few minutes (R = Ph) or 24 hours (R = Et)) to form 'silyl dihydride' complexes that are stable towards H₂ elimination.^{31,33}

At room temperature, compounds **2a–b** gave rise to a single hydride signal in the ¹H NMR spectrum and one broad ³¹P{¹H} NMR signal. However, upon cooling to 176 K, three ¹H NMR signals (**2a**: 5:5:2, **2b**: 4:4:3 relative integration) were observed in the low-frequency (<0 ppm) region, and the ³¹P{¹H} NMR spectrum contained one intense and three low intensity peaks (see Fig. 1 for **2a**), indicative of a major and a minor isomer (*vide infra*).



Scheme 1 Top: Synthesis of manganese germylene-hydride complexes [(dmpe)₂MnH(=GeR₂)] (**1a**: R = Ph, **1b**: R = Et). Bottom: Equilibria observed between germylene-hydride complex [(dmpe)₂MnH(=GeHⁿBu)] (**1c**) and the Mn(I) germyl complexes *trans*-[(dmpe)₂Mn(GeH₂ⁿBu)(HGeH₂ⁿBu)] and *mer*-[(dmpe)₂MnH(GeH₂ⁿBu)₂] upon exposure to excess hydrogermane.²⁹

Scheme 2 Reactions of the germylene-hydride complexes [(dmpe)₂MnH(=GeR₂)] (**1a**: R = Ph, **1b**: R = Et) with dihydrogen to afford an equilibrium mixture containing isomers of [(dmpe)₂MnH₂(GeHR₂)] (**2a**: R = Ph, **2b**: R = Et). The major isomer of **2a–b** was identified as the *trans*-hydrogermane hydride complex *trans*HGe-**2a,b**. For consistency with previous literature, the hydrogermane ligand in this isomer is drawn as a σ-complex, despite existing on a continuum between a sigma complex and a germyl dihydride species resulting from Ge–H bond oxidative addition.³⁹ The minor isomer of **2a–b** is tentatively assigned as the *cis* germyl dihydrogen complex *cis*-[(dmpe)₂Mn(GeHR₂)(H₂)] (*cis*-**2a–b**), possibly in rapid equilibrium with a small amount of the germanate complex [(dmpe)₂Mn(H₂GeHR₂)] (*central*-**2a–b**; shown in gray; *vide infra*). The inset shows *trans*H₂ isomers which were not experimentally observed.

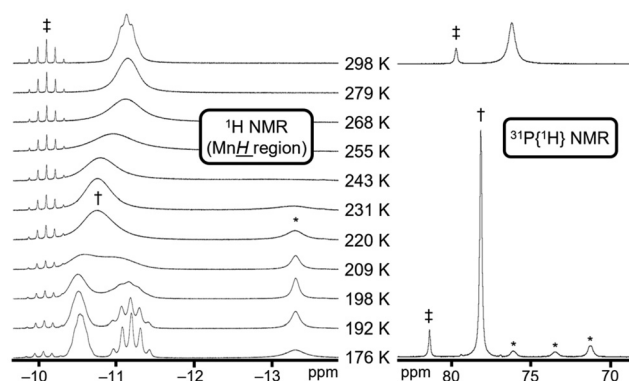


Fig. 1 Variable temperature ^1H NMR (500 MHz; left) and $^{31}\text{P}\{^1\text{H}\}$ NMR (202 MHz; right) spectra of the reaction mixture formed from the reaction of $[(\text{dmpe})_2\text{MnH}(\text{=GePh}_2)]$ (**1a**; †) with H_2 in d_8 -toluene (see Fig. S23† for $^{31}\text{P}\{^1\text{H}\}$ NMR spectra at all temperatures). This reaction affords the 'germyl dihydride' complex $[(\text{dmpe})_2\text{MnH}_2(\text{GeHPh}_2)]$ (**2a**), as a mixture of rapidly exchanging isomers, in slow equilibrium with **1a** and H_2 . Peaks attributed to *transHGe-2a* are indicated with the symbol †, whereas those for an isomer with a disphenoidal arrangement of the dmpe ligands (tentatively identified as *cis-2a*, possibly in rapid equilibrium with a small amount of *central-2a-b*; vide infra) are indicated with the symbol *.

The dominant isomer of **2a-b** in solution (84% for **2a**, 71% for **2b**) is the *trans*-hydrogermane hydride complex *trans*- $[(\text{dmpe})_2\text{MnH}(\text{HGeHR}_2)]$ (*transHGe-2a*: $\text{R} = \text{Ph}$, *transHGe-2b*: $\text{R} = \text{Et}$). At 176 K, this isomer gave rise to a single sharp peak in the $^{31}\text{P}\{^1\text{H}\}$ NMR spectrum (at 78 ppm (**2a**) or 76 ppm (**2b**)), indicative of an equatorial arrangement of the two dmpe ligands, and requiring rapid rotation of the hydrogermane ligand (which could alternatively be viewed as a hydride and a germyl ligand that are closely interacting) on the NMR time-scale. ^1H NMR signals for the major isomer include a single terminal GeH peak at 6.1 (**2a**) or 4.6 (**2b**) ppm, accompanied by two low frequency signals (−10.5 and −11.2 ppm for **2a**, −11.0 and −11.3 ppm for **2b**). In each case, the lower frequency signal is a well-defined quintet ($^2J_{\text{H,P}} = 56\text{--}58$ Hz) arising from the hydride ligand *trans* to the hydrogermane (positioned *cis* to four equivalent phosphines), whereas the higher frequency signal corresponds to the H atom of the manganese-coordinated Ge–H bond.

At 176 K, the lower symmetry isomer of **2a-b** gave rise to single MnH (−13.3 (**2a**) or −13.9 (**2b**) ppm) and terminal GeH (6.05 (**2a**) or 4.55 (**2b**) ppm) ^1H NMR environments integrating to 2H and 1H, respectively, and three $^{31}\text{P}\{^1\text{H}\}$ NMR signals with 1 : 1 : 2 integration, indicative of a disphenoidal arrangement of the phosphine donors (71–76 (**2a**) or 72–75 (**2b**) ppm). These data are consistent with two potential isomers: (a) *cis*- $[(\text{dmpe})_2\text{Mn}(\text{GeHR}_2)(\text{H}_2)]$ (*cis-2a-b*) containing *cis*-disposed dihydrogen and germyl ligands, or (b) $[(\text{dmpe})_2\text{Mn}(\text{H}_2\text{GeHR}_2)]$ (*central-2a-b*) featuring an anionic germanate ($\text{H}_2\text{GeHR}_2^-$) ligand that coordinates to manganese *via* the two newly-formed Ge–H bonds (the germanate ligand could alternatively be viewed as a germyl ligand interacting closely with two flanking hydride ligands). X-ray crystal structures have been

reported for Ru⁴⁰ and Nb⁴¹ complexes existing as germyl dihydrogen or germyl dihydride complexes, similar to the *cis* and *central* isomers of **2a-b**, respectively.

Maintaining a solution containing **1b** and **2b** in hexanes under an atmosphere of dihydrogen at −78 °C afforded crystals of *trans*- $[(\text{dmpe})_2\text{MnH}(\text{HGeHEt}_2)]$ (*transHGe-2b*) co-crystallized with the germylene-hydride starting material $[(\text{dmpe})_2\text{MnH}(\text{=GeEt}_2)]$ (**1b**) in a 0.46 : 0.54 ratio (Fig. 2). To the best of our knowledge, this is the first X-ray crystal structure of a hydrogermane manganese complex, and a rare example of a monometallic transition metal complex featuring a terminal hydrogermane ligand.^{39,42–45} However, due to co-crystallization of **1b** with *transHGe-2b* as well as disorder in the hydrogermane ligand in *transHGe-2b* (which together results in three overlapping Ge ellipsoids), the structure is only suitable to establish connectivity.

DFT calculations (ADF/AMS, gas phase, all-electron, TZ2P, PBE, ZORA, D3-BJ) were carried out on the aforementioned *transHGe*, *cis*, and *central* isomers of germyl dihydride complexes **2a-b**, as well as an isomer with *trans*-disposed H_2 and germyl ligands, *trans*- $[(\text{dmpe})_2\text{Mn}(\text{GeHR}_2)(\text{H}_2)]$ (*transH₂-2a-b*); Fig. 3 and S175, Table S13.† These calculations identified *transHGe-2a-b* (the major species observed in solution by NMR spectroscopy) as the global minimum, and $\Delta G_{176\text{K}}$ (176 K is the lowest temperature at which decoalesced NMR spectra were obtained) for conversion of *transHGe-2a-b* to the other isomers was 9–11 kJ mol^{−1} for *cis-2a-b* and *central-2a-b*, and 14–16 kJ mol^{−1} for *transH₂-2a-b* (Fig. 4).

The calculated structures of *transHGe-2a-b* feature a hydrogermane ligand which has undergone substantial but incomplete Ge–H bond oxidative addition. The terminal Mn–H, bridging Mn–H (bridging between Mn and Ge), and terminal Ge–H distances are 1.54–1.55, 1.56–1.57, and 1.58 Å, with Mayer

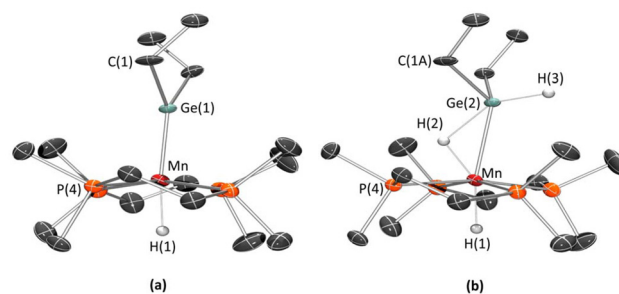


Fig. 2 Views of the (a) $[(\text{dmpe})_2\text{MnH}(\text{=GeEt}_2)]$ (**1b**) and (b) *transHGe-2b* components in crystals containing both of these species. The germanium-containing ligand in the structure is disordered over three parts – the germylene (GeEt_2) ligand in **1b** (54.2(3)% occupancy; view a), the hydrogermane (HGeHEt_2) ligand in *transHGe-2b* (40.2(3)% occupancy; view b), and another orientation of the hydrogermane ligand in *transHGe-2b* with 5.6(3)% occupancy (not shown; H atoms on this minor disorder component were not located from the difference map). Most hydrogen atoms have been omitted for clarity, with the exception of those on Mn and Ge which were located from the difference map and refined isotropically. Ellipsoids are shown at 50% probability.

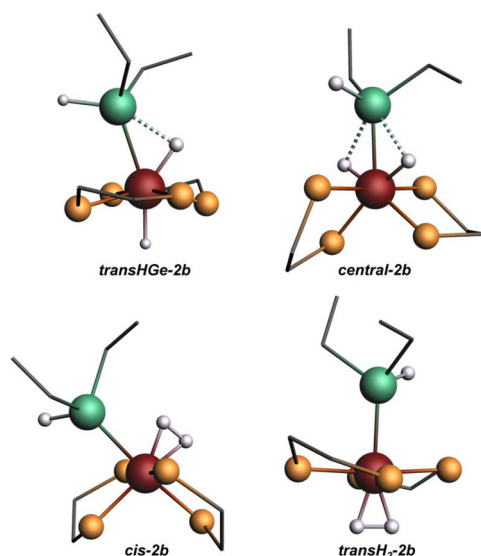


Fig. 3 Geometry optimized DFT calculated structures for the *transHGe*, *central*, *cis*, and *transH₂* isomers of $[(\text{dmpe})_2\text{MnH}_2(\text{GeHEt}_2)]$ (**2b**), with *P*-methyl groups and most hydrogen atoms omitted for clarity. Spheres represent Mn (red), Ge (green), P (orange), and H (white), whereas carbon atoms are represented by grey vertices. Solid bonds are those with Mayer bond orders >0.40 , while dashed bonds are those with Mayer bond orders between 0.13 and 0.23.

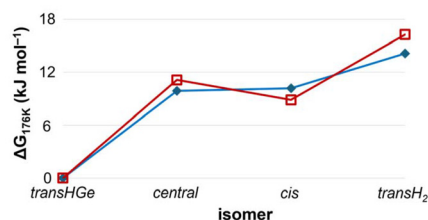


Fig. 4 DFT calculated Gibbs free energy changes (at 176 K) for isomerization of *trans*- $[(\text{dmpe})_2\text{MnH}(\text{HGeHR}_2)]$ (*transHGe-2a*: R = Ph, *transHGe-2b*: R = Et) to the *central*, *cis* and *transH₂* isomers. Values for **2a** are shown as red hollow squares, and values for **2b** are shown as blue diamonds.

bond orders of 0.82–0.83, 0.65, and 0.84 respectively, and the bridging Ge–H distances are 2.00–2.08 Å with Mayer bond orders of 0.22–0.23 (Fig. 5; left). These bridging Ge–H distances are similar to those in Mo (2.08(6) Å),³⁹ Rh (2.13(3) Å),⁴² and Pd (2.04(8) Å)⁴³ complexes that are described as σ -hydrogermane complexes with partial Ge–H bond oxidative addition. By contrast, they are elongated relative to those in a cationic Pt(II) σ -hydrogermane complex (XRD: 1.78(4) Å, DFT: 1.79 Å) which would be expected to feature very limited Ge–H bond oxidative addition.⁴⁴ Conversely, they are shorter than the Ge–H distances (2.17(4)–2.23(6) Å) in a series of nickel complexes described as containing germlyl and hydride ligands with a significant interligand interaction.³⁷

The Mn–Ge distances in *transHGe-2a-b* are 2.43 and 2.46 Å, with Mayer bond orders of 0.74 and 0.78 (Fig. 5). These

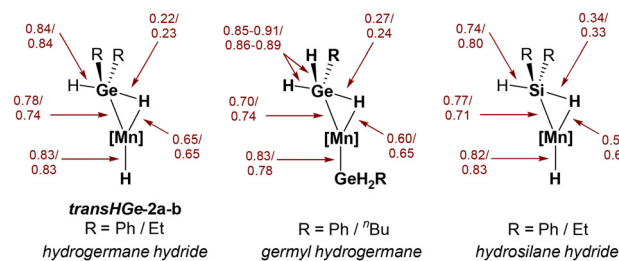


Fig. 5 Mayer bond orders for Mn–E, Mn–H and E–H bonds (E = Ge or Si) in *trans*- $[(\text{dmpe})_2\text{MnH}(\text{HGeHR}_2)]$ (*transHGe-2a-b*) compared with those previously reported for the germlyl hydrogermane complexes *trans*- $[(\text{dmpe})_2\text{Mn}(\text{GeH}_2\text{R})(\text{HGeH}_2\text{R})]$ (R = Ph or ⁿBu)²⁹ and the hydrosilane hydride complexes *trans*- $[(\text{dmpe})_2\text{MnH}(\text{HSiHR}_2)]$ (R = Ph or Et).³³ In all cases [Mn] is $\text{Mn}(\text{dmpe})_2$, and the same computational method (ADF/AMS, gas phase, all-electron, TZ2P, PBE, ZORA, D3-BJ) was employed.

bond distances are significantly longer than that in germlyl complex **1a** (2.2636(4) Å),²⁹ but are comparable with those calculated for the three higher energy isomers (the *cis*, *central* and *trans-H₂* isomers) of **2a-b**; 2.39–2.49 Å, with Mayer bond orders of 0.69–0.85 (Table S13[†]). They are also similar to the crystallographically determined Mn–Ge distances in the germlyl complexes $[(\text{dmpe})_2\text{Mn}(\text{GeHR}_2)(\text{L})]$ (R = Ph or Et, L = CNR or N₂) discussed below (2.475(1)–2.538(9) Å). Similarities between the transition metal–germanium distances in germlyl and hydrogermane complexes have previously been reported. For example, DFT calculations on $[(\kappa^2\text{-H}_2\text{PCH}_2\text{CH}_2\text{PH}_2)_2\text{Mo}(\text{CO})(\text{L})]$ (L = hydrogermane or germlyl hydride) complexes afforded Mo–Ge distances that are marginally longer in the germlyl hydride isomers (by 0.01–0.04 Å) than in the lowest energy hydrogermane isomers.³⁹

In Fig. 5, relevant Mayer bond orders in *transHGe-2a-b* are compared with those in the germlyl hydrogermane complexes *trans*- $[(\text{dmpe})_2\text{Mn}(\text{GeH}_2\text{R})(\text{HGeH}_2\text{R})]$ (R = Ph or ⁿBu),²⁹ and the hydrosilane hydride complexes *trans*- $[(\text{dmpe})_2\text{MnH}(\text{HSiHR}_2)]$ (R = Ph or Et).³³ These comparisons reveal (a) very similar Mn–H, Mn–Ge and Ge–H bond orders in *transHGe-2a-b* and the germlyl hydrogermane complexes, and (b) lower E–H_{Mn} (E = Ge or Si) bond orders in *transHGe-2a-b* compared to the hydrosilane hydride analogues (especially considering that the Mayer bond orders are marginally higher for the Ge–H *versus* Si–H bonds in free H₂GeEt₂ and H₂SiEt₂, respectively; 0.92 *vs.* 0.91), indicative of a greater degree of E–H bond oxidative addition in *transHGe-2a-b*. The trend in the relative degree of Si–H *vs.* Ge–H oxidative addition mirrors that previously noted for $[(\text{bisphosphine})_2\text{Mo}(\text{CO})(\text{HER}_3)]$ (E = Si, Ge) complexes.³⁹ The structures of the silicon analogues of *transHGe-2a-b* provide an important reference point given that the negative $J_{^{29}\text{Si},^1\text{H}}$ coupling constants for these complexes (–41 and –54 Hz; determined using ²⁹Si-edited ¹H–¹H COSY NMR spectroscopy) are indicative of dominant ¹J coupling (rather than ²J coupling which would give rise to a positive coupling constant), supporting the non-classical nature of the complexes; $J_{^{29}\text{Si},^1\text{H}}$ values ranging from 0 to –70 Hz are commonly considered to indicate activated Si–H bonds in nonclassical hydrosilane complexes.^{46–48}



Reactions with D₂

On a timescale of hours, reactions of $[(\text{dmpe})_2\text{MnH}(\text{=GeR}_2)]$ (**1a–b**) with D₂ in C₆D₆ or *d*₈-toluene cleanly produced $[(\text{dmpe})_2\text{MnD}_2(\text{GeHR}_2)]$ (**d₂-2a**: R = Ph, **d₂-2b**: R = Et), with hydrogen located exclusively in the terminal GeH bond in both (or all) isomers of the complexes. This reactivity with D₂ is analogous to that of the silylene complex $[(\text{dmpe})_2\text{MnH}(\text{=SiEt}_2)]$,³¹ and suggests that the formation of **2a–b** proceeds *via* initial isomerization of **1a–b** to a 5-coordinate germyl intermediate $[(\text{dmpe})_2\text{Mn}(\text{GeHR}_2)]$ (**A**), followed by H₂/D₂ oxidative addition. This contrasts the reactivity of D₂ with the heterobimetallic μ -germylene hydride complex $[(\text{OC})\text{Rh}(\mu\text{-H})(\mu\text{-dppm})_2(\mu\text{-GePh}_2)\text{Ir}(\text{CO})]^+$, which occurred rapidly at room temperature to generate $[(\text{OC})\text{Rh}(\mu\text{-H})(\mu\text{-dppm})_2(\mu\text{-GeDPh}_2)\text{IrD}(\text{CO})]^+$ as the primary product (although an equal distribution of H/D across all three sites was reported after 2 days at room temperature).³⁵

After 3 days in *d*₈-toluene, the reaction of **1a** with D₂ (4–6 equiv.) to form **d₂-2a** is at or near equilibrium, and low temperature $^{31}\text{P}\{^1\text{H}\}$ NMR spectroscopy revealed that the fast equilibrium between the major *transHGe* isomer† and the minor species (the *cis* or *central* isomer, or a rapidly exchanging mixture of both) is shifted further towards the minor species compared with the reaction with H₂ to form **2a**, affording an equilibrium isotope effect (EIE = $K_{\text{H}}/K_{\text{D}}$) of 0.63–0.69 over the temperature range 176–198 K. Room temperature H/D scrambling (between the Ge–H and Mn–D positions in $[(\text{dmpe})_2\text{MnD}_2(\text{GeHR}_2)]$) was not observed for **d₂-2a**, but heating overnight at 55–60 °C afforded baseline MnH¹³⁴ signals (<2% relative to the GeH signals).

By contrast, allowing the reaction of **1b** with D₂ (4 equiv.) to proceed for 4 days in *d*₈-toluene at room temperature afforded **d₂-2b** as well as other isotopologues (**d₃-2b**, and smaller amounts of **d₁-2b** and **2b**), giving rise to both GeH and MnH signals in the ¹H NMR spectrum, as well as some HD and H₂. These observations are consistent with slow hydrogermane (e.g. HDGeEt₂) dissociation and re-coordination from **d_n-2b** (perhaps from the *transHGe* isomer) as well as pathways involving D₂/HD/H₂ dissociation and re-coordination.

A low temperature (176 K) $^1\text{H}\{^{31}\text{P}\}$ NMR spectrum of the mixture of **2b**, **d₁-2b**, **d₂-2b**, and **d₃-2b** features a 1 : 1 : 1 triplet at –13.94 ppm overlapping with a broad singlet at slightly higher frequency (Fig. 6). These signals correspond to the minor isomer of **d_n-2b** (*n* = 0–2), and the coupling constant for the 1 : 1 : 1 triplet is 28 Hz, indicative of an HD ligand.^{49,50} This signal is proposed to arise from the *cis* isomer of $[(\text{dmpe})_2\text{Mn}(\text{GeXEt}_2)(\text{HD})]$ {X = D (**d₂-2b**) and H (**d₁-2b**); see Fig. 6}, and the 28 Hz coupling constant almost exactly

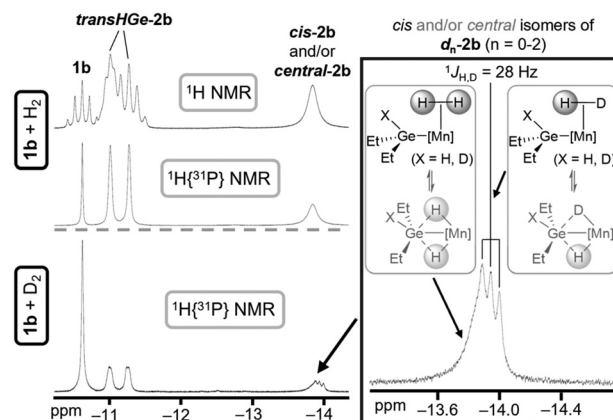


Fig. 6 ¹H and ¹H{³¹P} NMR spectra (176 K; 500 MHz) of the mixtures formed from the room temperature reactions of $[(\text{dmpe})_2\text{MnH}(\text{=GeEt}_2)]$ (**1b**) with (top) H₂ or (bottom) D₂ in *d*₈-toluene after 4 days. The reaction with D₂ afforded a mixture of **d₂-2b** and **d₃-2b**, as well as smaller amounts of **d₁-2b** and **2b**. Only the low frequency region of the spectra is shown (which does not contain any signals for **d₃-2b** or isomers/isotopomers of **d₂-2b** with a terminal Ge–H bond). The expansion on the right shows the low-frequency ¹H{³¹P} signal for the minor isomer(s) of **d_n-2b** (*n* = 0–2), which consists of a 1 : 1 : 1 triplet overlapping with a broad singlet. The 1 : 1 : 1 triplet is proposed to arise from isomers containing an HD ligand (**d₂-2b** where X = D and **d₁-2b** where X = H; X is the terminal H/D substituent on germanium), while the broad singlet is proposed to arise from isomers containing an H₂ ligand (**d₁-2b** where X = D and **2b**). The H₂ and HD complexes (*cis* isomers) may or may not be in rapid equilibrium with a small amount of a germanate species (*central* isomers). [Mn] = (dmpe)₂Mn.

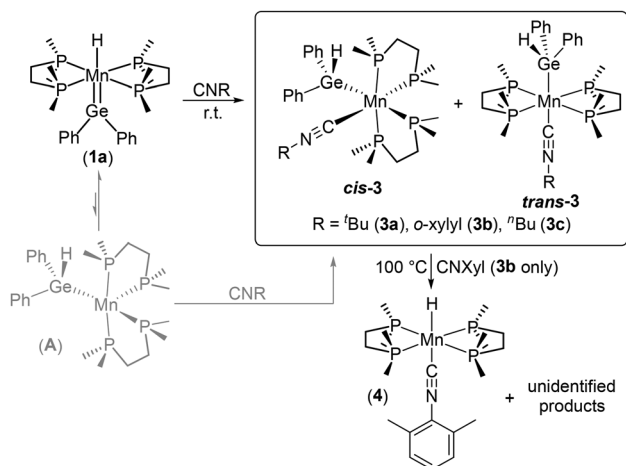
matches that predicted^{49,51} based on the calculated H–H distance of 0.95 Å in *cis*-**2b**. The aforementioned broad singlet is proposed to arise from the *cis* isomer of $[(\text{dmpe})_2\text{Mn}(\text{GeXEt}_2)(\text{H}_2)]$ {X = D (**d₁-2b**) and H (**2b**)}, both of which contain an H₂ ligand (see Fig. 6).

While these data suggest that the minor isomer of **2b** is the *cis*-dihydrogen complex (the *cis* isomer) rather than a germanate complex (the *central* isomer), the presence of a small amount of the *central* isomer (in rapid equilibrium with the *cis* isomer) cannot be excluded, given (a) the very similar energies of the *cis* and *central* isomers of **2a–b** in DFT calculations, and (b) potential differences in the position of any *cis*–*central* equilibrium in reactions involving HD *versus* H₂ or D₂ (especially considering that low-temperature reactions with H₂/D₂ to form an H₂/D₂ complex typically exhibit a substantial inverse equilibrium isotope effect).^{52,53} This situation contrasts that for silicon analogues of **2a–b**, where the spectroscopically identified isomers were *trans*- $[(\text{dmpe})_2\text{MnH}(\text{HSiHRR}')] (a \text{ } transHSi \text{ isomer})$ and the silicate complex $[(\text{dmpe})_2\text{Mn}(\text{H}_2\text{SiHRR}')] (a \text{ } central \text{ isomer})$, both of which were crystallographically characterized.³¹

Reactions with isonitriles

The putative 5-coordinate germyl intermediate $[(\text{dmpe})_2\text{Mn}(\text{GeHR}_2)]$ (**A**) was trapped using isonitriles. For example, exposure of $[(\text{dmpe})_2\text{MnH}(\text{=GePh}_2)]$ (**1a**) to an excess of *tert*-

† The ³¹P NMR signal for *transHGe*- $[(\text{dmpe})_2\text{MnD}(\text{DGeHPh}_2)]$ (**d₂-transHGe-2a**) is shifted 0.4 ppm to higher frequency than in the protio isotopomer *transHGe-2a*. This is relatively unusual, since secondary NMR isotopic shifts usually proceed to lower frequency upon substitution of a nearby atom with a heavier isotope.¹³⁴ The average ³¹P NMR environment observed at 298 K for all isomers of **2a**, as well as ³¹P NMR signals for the minor species in solution, are too broad for a similarly small secondary NMR isotopic shift to be measured.



Scheme 3 Syntheses of manganese(i) germyl isonitrile complexes $[(\text{dmpe})_2\text{Mn}(\text{GeHPh}_2)(\text{CNR})]$ (**3a–c**; $\text{R} = \text{tBu}$, Xyl or nBu) and the previously reported⁵⁴ hydride complex $[(\text{dmpe})_2\text{MnH}(\text{CNXyl})]$ (**4**). $\text{Xyl} = o\text{-xylyl}$.

butyl isonitrile (CN^tBu) afforded the germyl isonitrile complex $[(\text{dmpe})_2\text{Mn}(\text{GeHPh}_2)(\text{CNR})]$ (**3a**; $\text{R} = \text{tBu}$) as a yellow solid in 42% yield (Scheme 3). Analogues of **3a** featuring different isonitrile ligands (**3b**: $\text{R} = o\text{-xylyl}$, **3c**: $\text{R} = \text{nBu}$) were also synthesized *via* the same route (Scheme 3) and characterized *in situ* by NMR spectroscopy.[§] The reactions to form **3a–c** all proceeded to completion within 1 hour at room temperature.

In solution, two sets of NMR signals were observed for **3a–c** (Table S12[†]), consistent with a high symmetry *trans* isomer containing an equatorial belt of dmpe ligands (one $^{31}\text{P}\{^1\text{H}\}$ singlet was observed at 71–74 ppm), and a low symmetry *cis* isomer with multiple ^{31}P NMR environments arising from disphenoidal dmpe coordination. The GeH signals in the ^1H NMR spectra range from 5.06–5.27 ppm for the *trans* isomers and 5.45–5.48 for the *cis* isomers. Initially formed solutions of **3a–c** contain a mixture of *cis* and *trans* isomers in ratios ranging from 83:17 to 77:23, which remained unchanged overnight at room temperature (though a different ratio was observed in recrystallized samples of **3a** and **3c** due to preferential crystallization of the *cis* isomers).

[§]The reaction mixture formed from *n*-butyl isonitrile and **1a** contained a significant unidentified byproduct comprising ~30% of the mixture, which featured four $^{31}\text{P}\{^1\text{H}\}$ NMR environments and a very high frequency ^1H NMR signal (consistent with a $\text{CH}(\equiv\text{NR})^{135}$ or GeHR^{29} ligand). Removal of the solvent *in vacuo* followed by washing with hexanes and recrystallization from toluene layered with hexanes at -30°C resulted in isolation (though not with analytical purity) of *cis*-**3c**. Selected NMR data for the unidentified impurity are as follows: ^1H NMR (C_6D_6 , 600 MHz, 298 K, integrals normalized to 1H for the peak at 11.60 ppm): δ 11.60 (d of d, 1H, $J_{\text{H,P}}$ 9.3 and $J_{\text{H,P}}$ 3.6 Hz), 7.89, 7.79 (2 \times t, 2H, $J_{\text{H,H}}$ 7.1 Hz), 3.78, 3.59 (2 \times m, 1H), 1.46 (d, 3H, $J_{\text{H,P}}$ 4.8 Hz), 1.33 (d, 3H, $J_{\text{H,P}}$ 5.1 Hz), 1.29 (d, 3H, $J_{\text{H,P}}$ 6.4 Hz), 1.10 (d, 3H, $J_{\text{H,P}}$ 5.9 Hz), 0.82 (d, 3H, $J_{\text{H,P}}$ 4.6 Hz). $^{13}\text{C}\{^1\text{H}\}$ NMR (C_6D_6 , 151 MHz, 298 K): δ 159.42, 158.79, 134.23, 133.69, 127.78, 127.69, 126.32, 125.95, 58.58 (9 \times s), 35.79 (app. t, $J_{\text{C,P}}$ 22.1 Hz), 34.85 (d, $J_{\text{C,P}}$ 13.4 Hz), 33.88, 20.29 (2 \times m), 26.14 (d, $J_{\text{C,P}}$ 9.1 Hz), 25.74 (d of d, $J_{\text{C,P}}$ 12.8 and 6.9 Hz), 19.16 (d, $J_{\text{C,P}}$ 7.4 Hz). $^{31}\text{P}\{^1\text{H}\}$ NMR (C_6D_6 , 243 MHz, 298 K): δ 80.84, 72.74, 72.37, 62.64 (4 \times s, 1P).

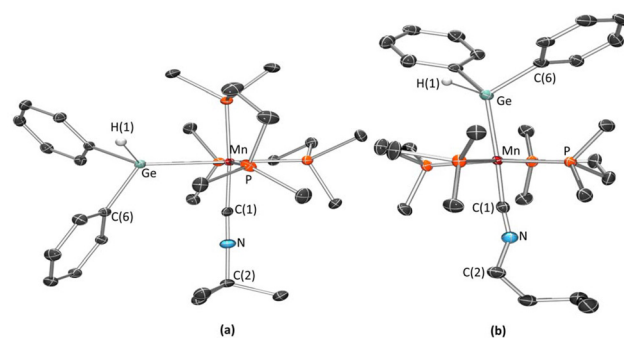


Fig. 7 X-ray crystal structures of (a) *cis*- $[(\text{dmpe})_2\text{Mn}(\text{GeHPh}_2)(\text{CN}^t\text{Bu})]$ (*cis*-**3a**) and (b) *trans*- $[(\text{dmpe})_2\text{Mn}(\text{GeHPh}_2)(\text{CN}^n\text{Bu})]$ (*trans*-**3c**), with ellipsoids at 50% probability. Most hydrogen atoms have been omitted for clarity, except for those on Ge, which were located from the difference map and refined isotropically.

Heating the reaction mixture from the synthesis of $[(\text{dmpe})_2\text{Mn}(\text{GeHPh}_2)(\text{CNXyl})]$ (**3b**; $\text{Xyl} = o\text{-xylyl}$) resulted in slow formation of the previously reported⁵⁴ manganese(i) hydride complex $[(\text{dmpe})_2\text{MnH}(o\text{-xylyl})]$ (**4**) (70% conversion after heating for ~12 h at 100°C) accompanied by unidentified byproducts; Scheme 3. Recrystallization from hexanes afforded X-ray quality crystals of **4**, with an Mn–H distance of 1.75(7) Å, an Mn–C distance of 1.789(6) Å, a C–N distance of 1.221(8) Å, and a C–N–C angle of $160.4(5)^\circ$ (Fig. S168[†]). An X-ray crystal structure of this complex was previously published⁵⁴ with a different unit cell (in a higher symmetry space group), featuring a perfectly straight Mn–C–N–C rod lying on a C_2 axis.

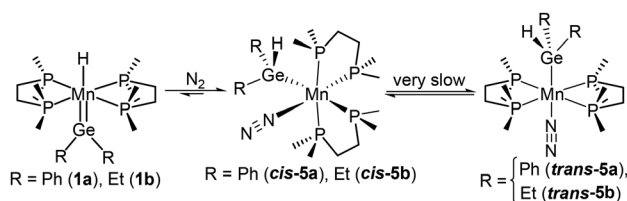
X-ray crystal structures were obtained for **3a–c**[¶] as the *cis* (**3a–b**) or *trans* (**3c**) isomer; Fig. 7 and S167, Table S11.[†] In all cases, the hydrogen atoms on Ge were located from the difference map and refined isotropically. The Mn–Ge distances of 2.475(1)–2.481(1) Å (*cis* isomers of **3a–b**) and 2.528(1) Å (*trans*-**3c**) are at the higher end of the range previously reported for neutral manganese(i) germyl complexes (2.37–2.53 Å),⁵⁵ and in each case, appreciable bending of the isonitrile ligands ($\text{C–N–C} = 144.9(4)\text{--}172.6(3)^\circ$) was observed.

Reactions with N_2

While coordination of the highly donating isonitrile ligands to manganese(i) is not unexpected, similar reactivity was also observed with dinitrogen. The manganese germylene-hydride complexes *trans*- $[(\text{dmpe})_2\text{MnH}(\equiv\text{GeR}_2)]$ (**1a**: $\text{R} = \text{Ph}$, **1b**: $\text{R} = \text{Et}$)²⁹ reacted in solution with dinitrogen (~1.5 atm) at room temperature to afford solutions of the germyl-dinitrogen complexes $[(\text{dmpe})_2\text{Mn}(\text{GeHR}_2)(\text{N}_2)]$ (**5a**: $\text{R} = \text{Ph}$, **5b**: $\text{R} = \text{Et}$); Scheme 4. These reactions are much slower than those involving isonitriles, reaching 95% (**5a**) or complete (**5b**) conversion

[¶]The X-ray crystal structure of **3b** contains two independent and essentially isostructural molecules in the unit cell. One of these has disorder in the dmpe ligands which could not be completely modelled from the difference map. Therefore, only bond metrics for **3b** from the molecule without disorder are included in the discussion and in Table S11.[†]





Scheme 4 Syntheses of manganese(i) germyl dinitrogen complexes $[(\text{dmpe})_2\text{Mn}(\text{GeHR}_2)(\text{N}_2)]$ (**5a**: R = Ph, **5b**: R = Et).

to **5a–b** after three days in the dark. Relative to the rich dinitrogen chemistry⁵⁶ of other d^6 transition metals such as Mo(0),⁵⁷ Fe(II),⁵⁸ and Re(I),⁵⁹ far fewer Mn(I)– N_2 complexes have been reported (see Scheme S1† and associated text).^{54,60–75}

In solution, a single set of NMR environments was observed for initially formed **5a** and **5b** (Table 1), consistent with a low symmetry *cis* isomer (featuring four distinct ^{31}P NMR environments). However, the diphenyl derivative $[(\text{dmpe})_2\text{Mn}(\text{GeHPh}_2)(\text{N}_2)]$ (**5a**) slowly isomerized to a higher symmetry *trans* isomer, affording a *cis*:*trans* ratio of ~3:1 after 3 days at room temperature in the dark (*i.e.* over the duration of the reaction of **1a** with N_2), and further conversion to achieve a 3:7 ratio occurred over an additional 12 days. Significant room temperature isomerization was not observed for the diethyl derivative $[(\text{dmpe})_2\text{Mn}(\text{GeHEt}_2)(\text{N}_2)]$ (**5b**) (upon complete consumption of **1b** after 3 days, only ~2% of the dinitrogen complex had isomerized to the *trans* isomer). However, the *trans* isomer became the dominant product after heating a solution of **5b** under an atmosphere of N_2 at 60 °C for 1 day. This indicates that for both **5a** and **5b**, the *trans* isomer is the thermodynamically favoured product. ^1H NMR spectra of **5a–b** feature GeH chemical shifts ranging from 3.02 to 5.04 ppm, where the values for each isomer of the diphenylgermyl derivative **5a** are 1.72–1.75 ppm higher frequency than those of **5b**, and the *cis* isomer GeH signal is shifted 0.63–0.66 ppm to higher frequency of the *trans* isomer in each case (Table 1).

In contrast to the *trans* isomer of the germyl isonitrile complexes **3a–c** and various other previously reported *trans*- $[(\text{dmpe})_2\text{MnRL}]$ complexes where the equatorial array of ^{31}P nuclei gave rise to a singlet,^{27,28,31,33,54} the $^{31}\text{P}\{^1\text{H}\}$ NMR signal arising from *trans*-**5a–b** was a very broad singlet (**5a**) or an approximately equal-intensity sextet (**5b**; left of Fig. 8) consistent with coupling to ^{55}Mn (nat. abund. = 100%; $I = 5/2$). Furthermore, the *trans* isomer of $[(\text{dmpe})_2\text{Mn}(\text{GeHEt}_2)(\text{N}_2)]$ (**5b**) afforded a quintet at –1094 ppm in the $^{55}\text{Mn}\{^1\text{H}\}$ NMR spectrum at ambient temperature (right of Fig. 8), indicative of a low electric field gradient at Mn. The manganese–phospho-

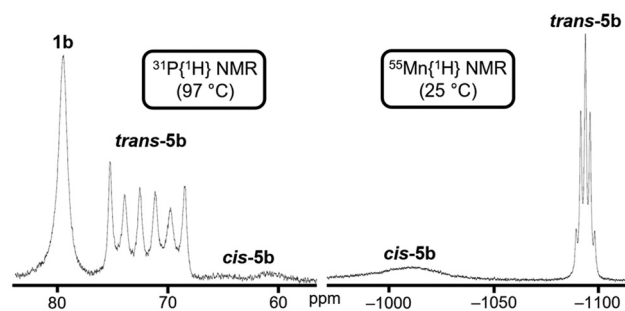


Fig. 8 $^{31}\text{P}\{^1\text{H}\}$ (left, 202 MHz) and $^{55}\text{Mn}\{^1\text{H}\}$ (right, 124 MHz) NMR spectra of $[(\text{dmpe})_2\text{Mn}(\text{GeHEt}_2)(\text{N}_2)]$ (**5b**) at 370 and 298 K, respectively (d_8 -toluene, N_2 atmosphere), showing the sextet or quintet arising from the *trans* isomer due to ^{31}P – ^{55}Mn coupling, along with peaks arising from the *cis* isomer and from (left only) *trans*- $[(\text{dmpe})_2\text{MnH}(\text{=GeEt}_2)]$ (**1b**; formed due to reversible N_2 dissociation from **5b** at elevated temperature). The $^{31}\text{P}\{^1\text{H}\}$ NMR spectrum was obtained at elevated temperature to reduce the extent of quadrupolar collapse for the *trans*-**5b** signal (note that signals for *cis*-**5b**, which are broadened at this temperature, are sharp singlets at low temperature as shown in Fig. S143† due to complete quadrupolar collapse of coupling to ^{55}Mn and/or slowing of a fluxional process which renders the ^{31}P atoms equivalent at high temperature).

rous coupling constant ($J_{^{31}\text{P},^{55}\text{Mn}}$) of 275 Hz in *trans*-**5b** is similar to those in previously reported alkyl tetracarbonyl manganese(i) complexes bearing a triphenylphosphine coligand (208–298 Hz).^{76,77} By contrast, *trans*-**5a** and *cis*-**5a–b** gave rise to broad singlets in the $^{55}\text{Mn}\{^1\text{H}\}$ NMR spectrum (Table 1), even upon heating to 97 °C.

Chemical shifts in ^{55}Mn NMR spectroscopy ($\delta_{^{55}\text{Mn}}$) vary widely for Mn(I) complexes.⁷⁸ For example, the trifluorophosphine complex $[(\text{F}_3\text{P})_5\text{MnH}]$ ⁷⁹ gave rise to a ^{55}Mn NMR signal at –2953 ppm, compared with +1077 ppm for $[\text{CpMn}(\eta^6\text{-cycloheptatriene})]$.⁸⁰ In this work, the ^{55}Mn chemical shifts for the *cis* and *trans* isomers of **5a–b** (–718 to –1094 ppm) fall near the centre of this range. The ^{55}Mn NMR signal for the diphenylgermyl derivative (**5a**) is 245–293 ppm more positive than the diethylgermyl derivative (**5b**), consistent with the trend previously noted for $[(\text{R}_3\text{Sn})\text{Mn}(\text{CO})_5]$, where $\delta_{^{55}\text{Mn}}$ for the triphenylstannyl derivative is 50 ppm more positive than for the trimethylstannyl derivative.⁸¹ The significant difference (79–127 ppm) in ^{55}Mn chemical shifts arising from *cis* and *trans* isomers in **5a–b** highlights the sensitivity of the ^{55}Mn nucleus to its electronic environment; similarly ^{55}Mn chemical shifts of –920 and –637 ppm have been reported for *trans* and *cis* isomers, respectively, of $[\text{ClMn}(\text{TeMe})_2(\text{CO})_3]$,⁸² and $\delta_{^{55}\text{Mn}}$ differences of up to 237 ppm have been reported for various diastereomers of manganese(i) carbonyl halide complexes bearing bidentate chalcogenoether ligands.^{82–85}

Solutions of **5a–b** in C_6D_6 are stable for days under an atmosphere of N_2 . However, in the absence of N_2 , these solutions

† The $^{55}\text{Mn}\{^1\text{H}\}$ NMR chemical shifts for *cis*-**5a**, *trans*-**5a**, *cis*-**5b** and *trans*-**5b** increase significantly as the temperature is increased, from –812, –991, –1070, and –1168 ppm, respectively, at 223 K, to –601, –730, –906, and –982 ppm, respectively, at 370 K. Below 272 K, the quintet arising from *trans*-**5b** begins to broaden significantly due to quadrupolar collapse. At elevated temperature, the $^{55}\text{Mn}\{^1\text{H}\}$ NMR spectra of **5a–b** also contain a peak arising from $[(\text{dmpe})_2\text{MnH}(\text{=GeR}_2)]$ (**1a–b**), which is in equilibrium with **5a–b** due to reversible N_2 dis-

sociation. At 370 K, the $^{55}\text{Mn}\{^1\text{H}\}$ NMR signals arising from **1a–b** are broad singlets at –1107 ppm for **1a** and –1226 ppm for **1b** (at 298 K, the signals are shifted to –1176 and –1303 ppm, respectively).

Table 1 Selected NMR spectroscopic data for dinitrogen complexes $[(\text{dmpe})_2\text{Mn}(\text{GeHR}_2)(\text{N}_2)]$ (**5a**: R = Ph, **5b**: R = Et) and $[(\text{dmpe})_2\text{Mn}(\text{SiHPh}_2)(\text{N}_2)]$ (**6**). $T = 298\text{ K}$; δ and J are in ppm and Hz, respectively; the solvent is C_6D_6 unless otherwise specified; the ^1H NMR chemical shift is for the EH (E = Ge or Si) signal

E/R	<i>cis</i>			<i>trans</i>		
	$\delta(^1\text{H})_{\text{EH}}/J_{\text{Si,H}}$	$\delta(^{31}\text{P})$	$\delta(^{55}\text{Mn})$	$\delta(^1\text{H})_{\text{EH}}/J_{\text{Si,H}}$	$\delta(^{31}\text{P})$	$\delta(^{55}\text{Mn})/J_{\text{P,Mn}}$
Ge/Ph (5a)	5.40	72.0, 69.3, 68.7, 58.7	-718^a	4.74	70.6	-845^a
Ge/Et (5b)	3.65	75.5, 71.4, 65.4, 60.6	-1011^a	3.02	72.3	$-1094/275\text{ Hz}^a$
Si/Ph (6)	5.53/141 Hz	71.8, 68.5, 64.1, 58.7	-973	4.82/140 Hz	70.8	$-1098/270\text{ Hz}$

^a $^{55}\text{Mn}\{^1\text{H}\}$ data for **5a–b** was obtained in d_8 -toluene.

suffered from slow dinitrogen loss to re-form the germylene-hydride starting materials **1a–b**. This process occurred more rapidly for **5a** than **5b**; ~8% conversion back to germylene-hydride was observed in a sealed J-young tube under argon after 6 hours or 2 days in the dark, respectively. Dissociation of N_2 could also be promoted by exposure to light;^{86–89} after 6 hours under a medium pressure mercury vapour lamp, a sealed solution of **5b** in a J-young tube converted to a 1.7 : 1 mixture of **1b** and **5b**, accompanied by a small amount of decomposition to unidentified species.

Complexes **5a–b** were isolated in 54–58% yield as yellow solids by removal of solvent *in vacuo* in the dark (**5a–b** are stable *in vacuo* for short periods of time in the absence of light) followed by recrystallization at $-30\text{ }^\circ\text{C}$ under argon. Analytical purity was confirmed by combustion elemental analysis (EA) and 2D powder X-ray diffraction (PXRD), and no germylene-hydride starting material was detected by IR spectroscopy (Nujol mull). Diffractograms of the bulk solids indicated that **5a** was isolated as an approximate 1 : 3 ratio of the *cis* and *trans* isomers, whereas **5b** was isolated almost exclusively as the *cis* isomer. In the solid state, **5a–b** proved to be reasonably stable to dinitrogen loss when kept under an argon atmosphere. For example, no decomposition was observed for **5b** after 2 years in a sealed vial at $-30\text{ }^\circ\text{C}$ as measured by PXRD and EA.

X-ray crystal structures were obtained for both the *cis* and *trans* isomers of **5a** and **5b** (Fig. 9 and S169;† Table 2). These complexes are octahedral with end-on terminal dinitrogen ligands, and (in all cases except *trans-5a*) the hydrogen atom on Ge was located from the difference map and refined isotropically. The manganese–germanium distances of 2.4795(6)–2.538(9) Å are at the higher end of the range previously reported for neutral manganese(i) germyl complexes (2.37–2.53 Å),⁵⁵ and are similar to those in the isonitrile complexes **3a–b** (2.475(1)–2.528(1) Å). The Mn–N distances are somewhat longer in the *cis* isomers (1.841(2) and 1.822(2) Å) than the *trans* isomers (1.806(2) and 1.79(2) Å), but the N–N distances (1.120(4)–1.139(3) Å) in all four complexes are equal within 3 standard deviations. To the best of our knowledge, the only other crystallographically characterized examples of neutral Mn(i) complexes containing a terminal dinitrogen ligand are the cymantrene derivative $[\text{CpMn}(\text{CO})_2(\text{N}_2)]$ ⁹⁰ (Mn–N = 1.8418(4) Å; N–N = 1.1144(1) Å)⁹¹ and the octahedral tetraphosphine hydride complex *trans*- $[(\text{dmpe})_2\text{MnH}(\text{N}_2)]$ (Mn–N =

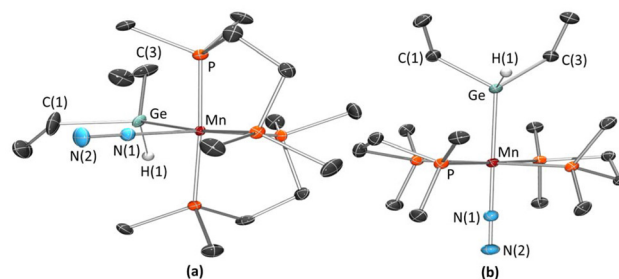


Fig. 9 X-ray crystal structures of (a) *cis*- $[(\text{dmpe})_2\text{Mn}(\text{GeHEt}_2)(\text{N}_2)]$ (*cis-5b*) and (b) *trans*- $[(\text{dmpe})_2\text{Mn}(\text{GeHEt}_2)(\text{N}_2)]$ (*trans-5b*), with ellipsoids at 50% probability. Most hydrogen atoms have been omitted for clarity, with the exception of those on Ge which were located from the difference map and refined isotropically. For *cis-5b*, the dmpe ligands are disordered over two positions, and only the dominant position (81.0(2)%) is shown.

1.817(5) Å; N–N = 1.127(7) Å),⁵⁴ which feature similar Mn–N and N–N distances to those in **5a–b**.

IR spectroscopy (Nujol mull) was employed as a more sensitive tool to investigate differences in Mn– N_2 bonding, and peaks were assigned to *cis* or *trans* isomers based on relative peak intensity (compared to expected ratios derived from PXRD). IR spectra of **5a–b** included $\nu(\text{N}\equiv\text{N})$ stretches at 2010, 1973, 1989, and 1968 cm^{-1} (calcd 2045, 2026, 2040, and 2018 cm^{-1}) for *cis-5a*, *trans-5a*, *cis-5b*, and *trans-5b*, respectively.** These data point to increased π -backdonation to N_2 in the *trans* complexes. The N–N stretches for both isomers of **5a–b** are lower than in previously reported cyclopentadienyl-containing (2078–2169 cm^{-1})^{64,66,90,92} and cationic (2146–2167 cm^{-1})^{73,74} manganese(i) complexes with terminal end-on N_2 ligands. However, they are slightly higher than in $[(\text{dmpe})_2\text{MnH}(\kappa^1\text{-N}_2)]$ ($\nu_{\text{N}\equiv\text{N}} = 1947\text{ cm}^{-1}$).⁵⁴ For broader comparison, the range of $\nu(\text{N}\equiv\text{N})$ values for end-on transition

IR spectroscopy $\nu_{\text{N}\equiv\text{N}}$ peaks for the two isomers of **5b overlap, and values reported here were obtained by peak fitting using Gaussian peak shapes and a quadratic baseline correction, which resulted in the lowest standard error and F statistic relative to alternative peak fitting methods using any combination of Gaussian, Voigt, or Gaussian/Lorentzian peak shapes, and zero, constant, linear, or quadratic background corrections (in all cases, $\nu_{\text{N}\equiv\text{N}}$ ranged from 1988–1989 cm^{-1} for the *cis* isomer and 1959–1968 cm^{-1} for the *trans* isomer).



Table 2 Selected X-ray crystallographic (and DFT calculated) bond metrics (Å or °) {and Mayer bond orders} for dinitrogen complexes [(dmpe)₂Mn(GeHR₂)(N₂)] (**5a–b**)

R	<i>cis</i>					<i>trans</i>				
	Mn–Ge	Mn–N	N≡N	Ge–Mn–N	Mn–N–N	Mn–Ge	Mn–N	N≡N	Ge–Mn–N	Mn–N–N
Ph (5a) ^a	2.4867(8) (2.51) {0.81}	1.841(2) (1.80) {1.01}	1.120(4) (1.14) {2.47}	85.95(7) (86.3)	176.2(2) (176.4)	2.538(9), 2.51 (1) (2.51) {0.87}	1.79(2) (1.79) {1.11}	1.14(3) (1.14) {2.45}	165.0(8), 169.7(8) (175.9)	177(2) (179.6)
Et (5b)	2.4795(6) (2.50) {0.80}	1.822(2) (1.80) {1.04}	1.124(3) (1.14) {2.48}	86.65(5) (86.6)	178.8(2) (178.2)	2.5089(9) (2.51) {0.86}	1.806(2) (1.79) {1.12}	1.139(3) (1.14) {2.43}	177.58(6) (177.4)	179.4(2) (178.9)

^a For *trans*-**5a**, two sets of values are provided for some bond metrics due to a 2-part disorder of the germyl ligand.

metal dinitrogen complexes typically spans from 2250 to 1800 cm^{−1} (cf. 2330 cm^{−1} for free N₂).⁵⁶

DFT calculations (ADF/AMS, gas phase, all-electron, TZ2P, PBE, ZORA, D3-BJ) were carried out to further probe the nature of Mn–N₂ bonding in **5a–b**. Geometry optimization of both the *cis* and *trans* isomers of **5a–b** afforded structures with Mn–Ge, Mn–N, and N–N distances within 0.04 Å of the crystallographically determined values, along with Ge–Mn–N and Mn–N–N angles within three standard deviations of the XRD metrics (with the exception of Ge–Mn–N in *trans*-**5a**, which involved a disordered germyl ligand in the X-ray crystal structure).

Mayer bond orders for the Mn–N and N≡N bonds in the *trans* isomers are 0.08–0.10 higher and 0.02–0.05 lower, respectively, than in the *cis* isomers (Table 2), indicative of increased π -backdonation in the former (*trans* isomers). This is consistent with the trend indicated by N–N stretching frequencies (*vide supra*), which are mirrored by the DFT calculated N≡N stretching frequencies which are 19–22 cm^{−1} lower for the *trans* isomers of **5a–b**.

Bonding between the N₂ ligands and (dmpe)₂Mn(GeHR₂) fragments was further investigated *via* fragment interaction calculations using the energy decomposition analysis (EDA)⁹³ method of Ziegler and Rauk (Table 3). This approach affords

an overall interaction energy, ΔE_{int} , which is divided into five components, as shown in eqn (1).^{94,95} In this analysis, ΔE_{elec} represents the electrostatic interaction energy (calculated using frozen charge distributions for both fragments), ΔE_{Pauli} corresponds to Pauli repulsion, ΔE_{orb} is the orbital interaction energy (this term includes all contributions resulting from intrafragment polarization), ΔE_{disp} is the dispersion interaction energy, and ΔE_{prep} is the energy needed to bring the fragments from their optimum geometries to their geometries in the unfragmented complex.

$$\Delta E_{\text{int}} = \Delta E_{\text{elec}} + \Delta E_{\text{Pauli}} + \Delta E_{\text{orb}} + \Delta E_{\text{disp}} + \Delta E_{\text{prep}} \quad (1)$$

Overall interaction energies for N₂ coordination are −117 (**5a**) and −149 (**5b**) kJ mol^{−1} for the *cis* isomers and −163 (**5a**) and −173 (**5b**) kJ mol^{−1} for the *trans* isomers. Stronger N₂ bonding to manganese in the *trans* isomers is driven by stronger electrostatic and orbital contributions (ΔE_{elec} and ΔE_{orb} are more negative by 17–19 and 31–32 kJ mol^{−1}, respectively), partially offset by increased Pauli repulsion (ΔE_{Pauli} is more positive by 30–32 kJ mol^{−1}). The less negative ΔE_{int} for the Mn–N₂ bond in *cis*-**5a** relative to *cis*-**5b** is driven primarily by a higher preparation energy for the (dmpe)₂Mn(GeHPh₂) fragment. This

Table 3 Fragment interaction calculation data for the *cis* and *trans* isomers of **5a–b** {(dmpe)₂Mn(GeHR₂) + N₂}. All energies are in kJ mol^{−1}, ΔE_{int} values are BSSE-corrected, and for ETS-NOCV data, values in parentheses are a percentage of ΔE_{orb} . Hirsh = fragment Hirshfeld charge, [M] = (dmpe)₂Mn(GeHR₂)

	GeHR ₂	<i>cis</i> - 5a GeHPh ₂	<i>trans</i> - 5a	<i>cis</i> - 5b GeHEt ₂	<i>trans</i> - 5b
EDA	ΔE_{int}	−117	−163	−149	−173
	ΔE_{elec}	−321	−338	−320	−339
	ΔE_{orb}	−391	−422	−395	−427
	ΔE_{Pauli}	545	575	540	572
	ΔE_{disp}	−15	−14	−14	−14
	ΔE_{prep}	57	28	32	26
	BSSE	9	9	9	9
Hirsh	[M]	0.29	0.34	0.31	0.35
	N ₂	−0.29	−0.34	−0.31	−0.35
ETS-NOCV	ΔE_{σ}	−118 (30%)	−119 (28%)	−119 (30%)	−114 (27%)
	$\Delta E_{\pi(1)}$	−129 (33%)	−138 (33%)	−131 (33%)	−142 (33%)
	$\Delta E_{\pi(2)}$	−116 (30%)	−133 (32%)	−119 (30%)	−139 (32%)
	Other	−28 (7%)	−32 (7%)	−27 (7%)	−32 (8%)



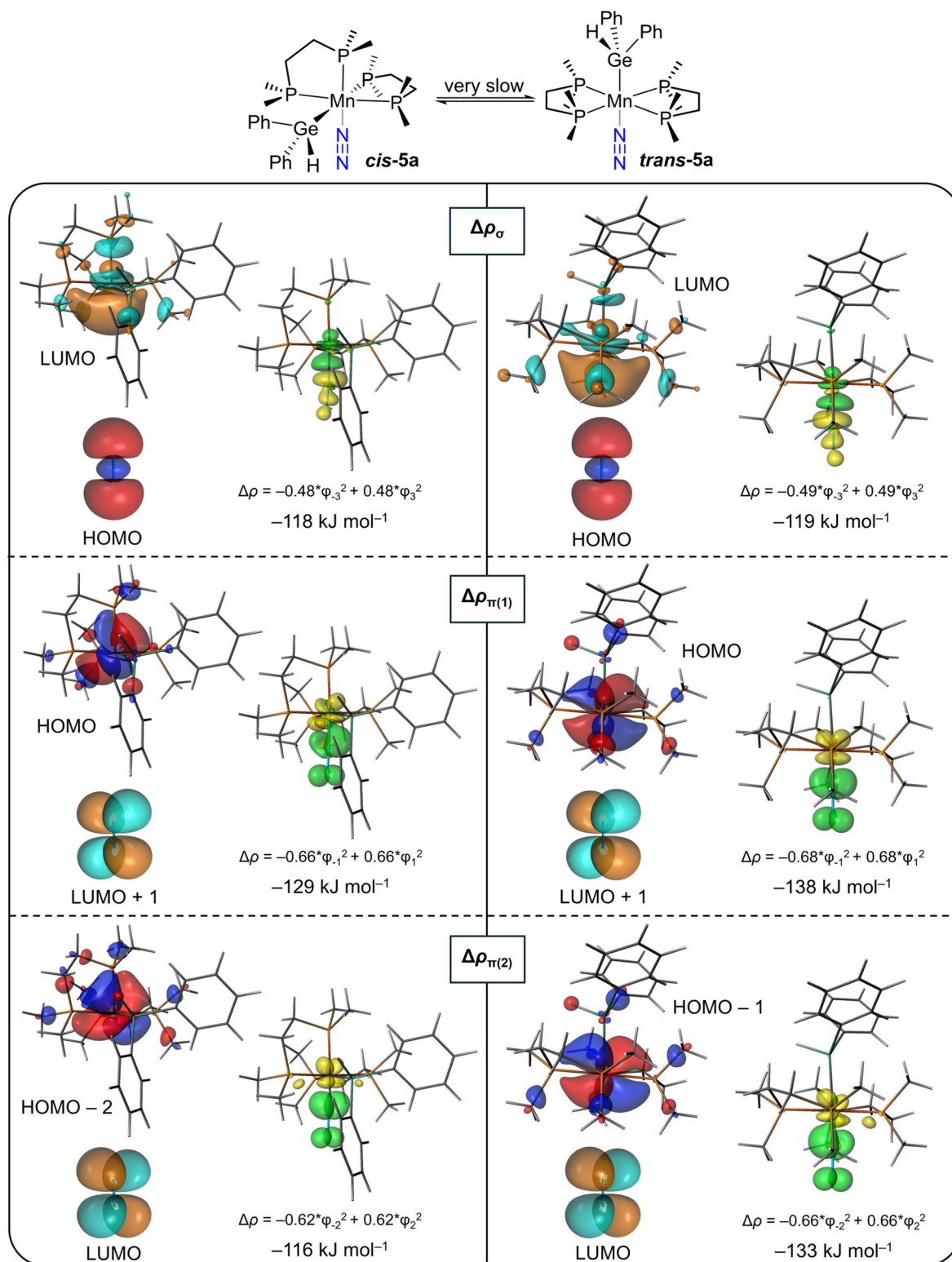


Fig. 10 Deformation density contributions (shown in green/yellow) and the main fragment orbital contributions (shown in red/blue or orange/turquoise) to bonding between a (dmpe)₂Mn(GeHPh₂) fragment and an N₂ fragment in the *cis*- (left) and *trans*- (right) isomers of [(dmpe)₂Mn(GeHPh₂)(N₂)] (**5a**). Three major interactions were observed ($\Delta\rho_\sigma$, $\Delta\rho_{\pi(1)}$ and $\Delta\rho_{\pi(2)}$). Deformation density isosurfaces (set to 0.003) correspond to increased (green) and decreased (yellow) electron density relative to the non-interacting fragments. Orbital isosurfaces are set to 0.03.



is due to stabilization of the geometry optimized fragment through a γ -hydride interaction involving an *ortho* C–H bond of a phenyl substituent on germanium (illustrated by a Mn...H bond distance of 1.91 Å and a Mayer bond order of 0.24; Fig. S176†).

The deformation density ($\Delta\rho$) associated with the orbital interaction component (ΔE_{orb}) from fragment interaction calculations was further divided using the Extended Transition State and Natural Orbitals for Chemical Valence (ETS-NOCV) method (Table 3), affording a textbook example of end-on N_2 bonding to a transition metal. Deformation density isosurfaces and the main fragment orbital contributors for the two isomers of **5a** are shown in Fig. 10 (similar figures for **5b**, and the NOCVs associated with each ETS-NOCV contribution, are shown in Fig. S179–182†). In each case, three contributions of similar energy (27–33% of ΔE_{orb} in all cases) were elucidated. One of these ($\Delta\rho_\sigma$) involves σ -donation from the HOMO of dinitrogen to the LUMO of the $(\text{dmpe})_2\text{Mn}(\text{GeHR}_2)$ fragment, whereas the other two contributions ($\Delta\rho_{\pi(1)}$ and $\Delta\rho_{\pi(2)}$) involve orthogonal π -backdonation from occupied manganese d orbitals to the vacant π^* orbitals of dinitrogen. The relative energies of these σ -donation and π -backdonation contributions are similar to those reported for other end-on N_2 complexes.^{96–100}

The aforementioned differences in the magnitude of ΔE_{orb} between the *cis* and *trans* isomers of **5a–b** is driven exclusively by the two π interactions, which are stronger (by 7–17 kJ mol^{−1}) in the *trans* isomers. More negative Hirshfeld charges on the N_2 fragment (from fragment interaction calculations) in the *trans* isomers (−0.34 to −0.35, versus −0.29 to −0.31 for the *cis* isomers; Table 3) also indicate an increase in charge transfer from the $(\text{dmpe})_2\text{Mn}(\text{GeHR}_2)$ fragment to N_2 , consistent with increased π -backdonation in the *trans* isomers.

Reaction of N_2 with $[(\text{dmpe})_2\text{MnH}(\text{=SiPh}_2)]$

Given that the germylene-hydride complexes (**1a–b**) reacted with N_2 , we were interested to probe whether a silylene-hydride analogue would engage in analogous reactivity. Indeed, $[(\text{dmpe})_2\text{MnH}(\text{=SiPh}_2)]$ (which exists in solution as an equilibrium mixture of the *cis* and *trans* isomers)³¹ also reacts with dinitrogen to afford complexes tentatively identified by NMR spectroscopy as *cis* and *trans* isomers of the silyl dinitrogen complex $[(\text{dmpe})_2\text{Mn}(\text{SiHPh}_2)(\text{N}_2)]$ (**6**); Scheme 5. This reactivity reflects that previously reported for another d⁶ silylene-

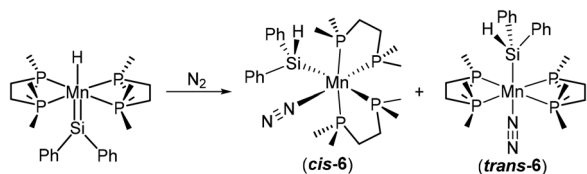
hydride complex, $[(\text{Cp}^*)(^i\text{Pr}_2\text{MeP})\text{FeH}(\text{=SiHTrip})]$, which reversibly coordinates N_2 .¹⁰¹

Unfortunately, the synthesis of the silylene-hydride starting material affords an inseparable mixture of this complex with the silyl dihydride species $[(\text{dmpe})_2\text{MnH}_2(\text{SiHPh}_2)]$ ³¹ (which does not react with N_2 under mild conditions), so complex **6** was generated as a mixture with $[(\text{dmpe})_2\text{MnH}_2(\text{SiHPh}_2)]$. X-ray quality crystals of **trans-6** (Fig. S170†) were obtained from this mixture, showing that **trans-6** is isostructural to the germyl derivative **trans-5a**, including statistically equivalent Mn–N and N–N distances. The Mn–Si distances of 2.457(3)–2.469(6) Å in **trans-6** are significantly elongated relative to those in the previously reported manganese(i) $\text{SiH}_n\text{R}_{3-n}$ ($n = 1–2$) complexes; the primary silyl complexes $[(\text{dmpe})_2\text{Mn}(\text{SiH}_2\text{R})(\text{CNR}')] (R = \text{Ph}, ^n\text{Bu}, R' = ^t\text{Bu}, o\text{-xylyl}; 2.3552(5)–2.3618(5) \text{ Å})$,³² and the more electron-poor tetracarbonyl phosphine complex $[(\text{OC})_4\text{Mn}(\text{SiHPh}_2)(\text{PPh}_3)]$ (2.410(1) Å).¹⁰²

Selected NMR spectroscopic data for **6** (Table 1) includes ¹H NMR SiH environments at 5.53 (*cis-6*, ¹J_{H,Si} = 141 Hz) and 4.82 (*trans-6*, ¹J_{H,Si} = 140 Hz and ³J_{H,P} = 8.6 Hz) ppm, and ²⁹Si NMR signals at 36.6 (*cis-6*) and 33.9 (*trans-6*) ppm. Similar to the NMR spectra of diethylgermyl derivative **5b**, the *cis* isomer of **6** gave rise to multiple ³¹P{¹H} NMR resonances and a broad singlet in the ⁵⁵Mn{¹H} NMR spectrum at −971 ppm, while **trans-6** afforded a single ³¹P{¹H} NMR signal at 70.8 ppm which shows coupling to ⁵⁵Mn in the process of quadrupolar collapse and a quintet in the ⁵⁵Mn{¹H} NMR spectrum at −1098 ppm (¹J_{Mn,P} = 270 Hz; Fig. S164 and S157†). The shift in ⁵⁵Mn NMR signals to more negative frequency (by 253–255 ppm) relative to those of germyl derivative **5a** mirrors the previously reported trend in the tetryl-ligated manganese(i) carbonyl complexes $[(\text{R}_3\text{E})\text{Mn}(\text{CO})_5]$ ($R = \text{Cl}, \text{C}_6\text{F}_5$, or Ph , $\text{E} = \text{Si}$ or Ge), where $\delta_{55\text{Mn}}$ is more negative (by 40–330 ppm) in the silyl derivatives.¹⁰³ However, this trend differs from those for manganese(i) complexes which vary in the identity of a halide^{82–84,104,105} or chalcogenoether^{82–84,106} ligand, where more negative ⁵⁵Mn chemical shifts were observed proceeding down the group.

Summary and conclusions

Reactions of the germylene-hydride complexes $[(\text{dmpe})_2\text{MnH}(\text{=GeR}_2)]$ ($R = \text{Ph}$ or Et ; **1a–b**) with H_2 afforded $[(\text{dmpe})_2\text{MnH}_2(\text{GeHR}_2)]$ (**2a–b**) in slow equilibrium with the starting materials. This reactivity contrasts that of the silicon analogues which reacted completely to form ‘silyl dihydride’ complexes that are stable towards H_2 elimination. In solution, complexes **2a–b** exist as multiple isomers in rapid equilibrium, which were characterized by low temperature NMR spectroscopy. The major isomer of **2a–b** is *trans*- $[(\text{dmpe})_2\text{MnH}(\text{HGeHR}_2)]$ (**transHGe-2a–b**) featuring *trans*-disposed hydride and hydrogermane ligands, and DFT calculations indicate a higher degree of Ge–H bond oxidative addition in **transHGe-2a–b** compared to Si–H bond oxidative addition in the previously reported hydrosilane hydride analogues *trans*- $[(\text{dmpe})_2\text{MnH}(\text{HSiHR}_2)]$. The minor isomer of **2a–b** features a



Scheme 5 Synthesis (*in situ*) of the manganese(i) silyl dinitrogen complex $[(\text{dmpe})_2\text{Mn}(\text{SiHPh}_2)(\text{N}_2)]$ (**6**) as a mixture of the *cis* and *trans* isomers. The starting material $[(\text{dmpe})_2\text{MnH}(\text{=SiPh}_2)]$ exists as a mixture of the *trans* (minor) and *cis* (major) isomers; only one isomer is shown.

disphenoidal arrangement of the phosphine donors, and is tentatively assigned as the *cis* germyl dihydrogen complex *cis*-[[dmpe]₂Mn(GeHR₂)(H₂)] (*cis*-**2a-b**); the presence of this isomer is supported by the observation of a 1 : 1 : 1 triplet with a large (28 Hz) *J*_{H,D} coupling constant in the low-temperature ¹H{³¹P} NMR spectrum of a mixture containing partially deuterated isotopologues of **2b** (where the triplet is attributed to [[dmpe]₂Mn(GeXEt₂)(HD)] {X = D (**d₂-2b**) and H (**d₁-2b**)}, both of which contain an HD ligand). However, the presence of a small amount of the germanate complex [[dmpe]₂Mn(H₂GeHR₂)] (*central*-**2a-b**), in rapid equilibrium with the *cis* isomer, cannot be excluded, given (a) the very similar energies of the *cis* and *central* isomers of **2a-b** in DFT calculations, and (b) potential differences in the position of any *cis*-*central* equilibrium in reactions involving HD *versus* H₂ or D₂.

An X-ray crystal structure was obtained for *trans*HGe-**2b** co-crystallized with the starting germylene complex **1b**. To the best of our knowledge, this is the first crystallographically characterized example of a manganese hydrogermane complex, and more generally, *trans*HGe-**2a-b** are rare examples of monometallic transition metal complexes featuring a terminal hydrogermane ligand. Reactions of **1a-b** with D₂ initially afforded only [[dmpe]₂MnD₂(GeHR₂)] (**d₂-2a-b**), suggesting that the formation of **2a-b** proceeds *via* initial isomerization of the germylene-hydride complexes to a 5-coordinate manganese (i) germyl intermediate [[dmpe]₂Mn(GeHR₂)] (**A**). This intermediate was trapped by reacting [[dmpe]₂MnH(=GePh₂)] (**1a**) with isonitriles to afford the germyl isonitrile complexes [[dmpe]₂Mn(GeHPh₂)(CNR)] (**3a-c**). These complexes were formed as mixtures of *cis* and *trans* isomers, and X-ray crystal structures were obtained for either isomer depending on the isonitrile used.

Germylene-hydride complexes **1a-b** also reacted slowly with dinitrogen to afford the manganese(i) germyl dinitrogen complexes [[dmpe]₂Mn(GeHR₂)(N₂)] (**5a-b**). Complexes **5a-b** were initially formed as *cis* isomers, but the *trans* isomer became dominant over time in solution (at room temperature or with mild heating). The N₂ ligands in **5a-b** are labile in solution, but the complexes are reasonably stable in the solid state. X-ray crystal structures were obtained for both isomers of **5a** and **5b**, providing rare examples of crystallographically characterized manganese(i) terminal N₂ complexes. The silylene complex [[dmpe]₂MnH(=SiPh₂)] was also shown to react with N₂ to form the silyl dinitrogen derivative [[dmpe]₂Mn(SiHPh₂)(N₂)] (**6**) as a mixture of *cis* and *trans* isomers.

Unusually, NMR spectra of *trans*-**5b** and *trans*-**6** showed 1-bond coupling between ³¹P (100% abundance, *I* = 1/2) and ⁵⁵Mn (100% abundance; *I* = 5/2), resulting in an approximate 1 : 1 : 1 : 1 : 1 : 1 sextet in the ³¹P{¹H} NMR spectra (at elevated temperature) and a 1 : 4 : 6 : 4 : 1 quintet in the ⁵⁵Mn{¹H} NMR spectra. Such coupling has not been observed in other [[dmpe]₂MnXL] (X = an anionic ligand; L = a neutral ligand) complexes. Bonding between Mn and N₂ was studied through XRD, IR spectroscopy, and DFT calculations (including ETS-NOCV analysis), revealing stronger N₂ coordination in the *trans* isomers. This results from larger electrostatic and orbital

contributions (Δ*E*_{elec} and Δ*E*_{orb}) to bonding, partly offset by increased Pauli repulsion (Δ*E*_{Pauli}), where the larger Δ*E*_{orb} stems from enhanced π-backdonation.

Experimental

General methods

An argon-filled MBraun UNILab glove box equipped with a −30 °C freezer was employed for the manipulation and storage of all oxygen- and moisture-sensitive compounds. Air-sensitive preparative reactions were performed on a double-manifold high-vacuum line equipped with a two stage Welch 1402 belt-drive vacuum pump (ultimate pressure 1 × 10^{−4} Torr) using standard techniques.¹⁰⁷ The vacuum was measured periodically using a Kurt J. Lesker 275i convection enhanced Pirani gauge. Residual oxygen and moisture was removed from the argon stream by passage through an Oxisorb-W scrubber from Matheson Gas Products.

Benzene was purchased from Sigma-Aldrich, hexanes and toluene were purchased from Caledon, and deuterated solvents were purchased from ACP Chemicals. Benzene, hexanes, and toluene were initially dried and distilled at atmospheric pressure from sodium/benzophenone (first two) or sodium (toluene). All solvents were stored over an appropriate drying agent (benzene, toluene, *d*₈-toluene, C₆D₆ = Na/Ph₂CO; hexanes = Na/Ph₂CO/tetraglyme) and introduced to reactions or solvent storage flasks *via* vacuum transfer with condensation at −78 °C.

Cl₂GePh₂, Cl₂GeEt₂, H₂SiPh₂, dmpe, 1,4-dioxane, ethylmagnesium chloride solution (2.0 M in diethyl ether), D₂, *tert*-butyl isonitrile, *o*-xylyl isonitrile, and *n*-butyl isonitrile were purchased from Sigma-Aldrich. Manganese dichloride was purchased from Strem Chemicals. [[dmpe]₂MnH(=GePh₂)] (**1a**),²⁹ [[dmpe]₂MnH(=GeEt₂)] (**1b**),²⁹ and [[dmpe]₂MnH(=SiPh₂)]³¹ were prepared according to literature procedures, as were reagents used in their preparation; [[dmpe]₂MnH(C₂H₄)]^{27,28} H₂GePh₂,¹⁰⁸ and H₂GeEt₂.²⁹ Argon, H₂, and N₂ were purchased from PraxAir.

NMR spectroscopy was performed on Bruker AV-500 and AV-600 spectrometers. Spectra were obtained at 298 K unless otherwise indicated. ¹H NMR spectra were referenced relative to SiMe₄ through a resonance of the protio impurity of the solvent: C₆D₆ (δ 7.16 ppm) and *d*₈-toluene (δ 2.08, 6.97, 7.01, and 7.09 ppm; at lower or higher temperatures the peak at 2.08 ppm was used). ¹³C NMR spectra were referenced relative to SiMe₄ through a resonance of the solvent: C₆D₆ (δ 128.06 ppm) and *d*₈-toluene (δ 20.43, 125.13, 127.96, 128.87, and 137.48 ppm; at lower temperatures the peak at 20.43 ppm was used). ²H NMR spectra were referenced through a resonance of the solvent C₆D₆ (δ 7.16 ppm) and the CD₃ peak in *d*₈-toluene (δ 2.08 ppm). The ²⁹Si, ³¹P, and ⁵⁵Mn NMR spectra were referenced to SiMe₄ (1 vol% in CDCl₃; δ = 19.867187%), 85% aqueous H₃PO₄ (δ = 40.480742%), and conc. KMnO₄(aq) (δ = 24.789218%), respectively, by indirect referencing from a ¹H NMR spectrum.¹⁰⁹ NMR chemical shift abbreviations: s =



singlet, d = doublet, t = triplet, q = quartet, quin. = quintet, m = multiplet, app. = apparent, br. = broad.

Combustion elemental analyses were performed at the University of Calgary.

IR spectroscopy was performed in a nujol mull sandwiched between CaF₂ plates using a ThermoScientific Nicolet iS5 spectrometer on transmission mode. Spectra collection and viewing was done using OMNIC.

Single-crystal X-ray crystallographic analyses were performed on crystals coated in Paratone oil and mounted on a STOE IPDS II diffractometer with an image plate detector or a Bruker Dual Source D8 Venture diffractometer using the I μ S 3.0 Mo source at 70 W with a HELIOS Mo focusing optic (ELM33) in the McMaster Analytical X-Ray (MAX) Diffraction Facility. A semi-empirical absorption correction was applied using redundant and symmetry related data. Raw data was processed using XPREP (as part of the APEX4 v2022.10-0 software), and solved by intrinsic (SHELXT)¹¹⁰ methods. Structures were completed by difference Fourier synthesis and refined with full-matrix least-squares procedures based on F^2 . In all cases, non-hydrogen atoms were refined anisotropically and hydrogen atoms were generated in ideal positions and then updated with each cycle of refinement (with the exception of hydrogen atoms on Ge and Mn, which were located from the difference map and refined isotropically). Refinement was performed with SHELXL¹¹¹ in Olex2.¹¹²

2D powder X-ray diffraction was performed on a Bruker D8 Discover diffractometer equipped with a Vantec 500 area detector and a focused Cu source with K α radiation ($\lambda = 1.54056$ Å) operated at 40 kV and 40 mA, or a Bruker D8 Venture diffractometer equipped with a PHOTON CMOS (complementary metal oxide semiconductor) area detector and a Incoatec I μ S Cu source with K α radiation ($\lambda = 1.54184$ Å) operated at 50 kV and 1.10 mA. The samples were packed in a 0.5 mm o.d. special glass (SG; wall thickness 0.01 mm) capillary tube for X-ray diffraction (purchased from Charles Supper Co.) and sealed by inverting to submerge the open end in a pool of Apiezon H-grease within the glovebox. The powder diffractograms were generated using Gadds and/or DiffraC.eva. Rietveld refinement (PV_TCHZ peak types between 5.5° and 35°, LP factor of 23.7, 6th order PO spherical harmonics for preferred orientation, and a Chebychev order 9 background) was performed using Topas.

All prepared complexes are air sensitive, and their products upon reaction with air are malodorous. Therefore, unless otherwise indicated, all syntheses were conducted under an atmosphere of argon.

DFT calculations

All calculated structures were fully optimized with the ADF/AMS DFT package (SCM, version 2020.102 for **2a–b** or 2024.102 for **5a–b**).^{113,114} For **2a–b**, energy minima were located for four (*transHGe* isomer) or three (*cis* and *central* isomers) rotamers, and only data from the minima leading to the lowest Gibbs free energy of formation at 176 K is discussed. Calculations were conducted in the gas phase within the generalized gradient approximation (GGA) using the 1996

Perdew–Burke–Ernzerhof exchange and correlation functional (PBE),¹¹⁵ the scalar zeroth-order regular approximation (ZORA)^{116–120} for relativistic effects, and Grimme's DFT-D3-BJ dispersion correction.^{121,122} Geometry optimizations were conducted using all-electron triple- ζ basis sets with two polarization functions (TZ2P), fine integration grids (Becke^{123,124} very-good), and stricter-than-default convergence criteria (gradients = 0.0001, step = 0.002). Calculations were restricted.

Visualization of the computational results was performed using the ADF/AMS-GUI (SCM) or Biovia Discovery Studio Visualizer. Orbitals and deformation densities were generated with a fine grid using the densf auxiliary program.

Analytical frequency calculations^{125–127} were conducted on all geometry optimized structures (including geometry optimized fragments) to ensure that the geometry optimization led to an energy minimum.

Bonding was analyzed in more detail using a fragment approach (energy decomposition analysis^{128,129} with ETS-NOCV analysis^{130–133}) that considered the interaction of neutral (dmpe)₂Mn(GeHR₂) fragments with neutral N₂ ligands. Fragments were generated from the TZ2P geometry optimized structures of each complex, geometries were frozen, and single-point calculations (as well as the EDA/ETS-NOCV calculations) were conducted using the same parameters as for the geometry optimizations. Preparation energies (ΔE_{prep}) were obtained for all fragments by allowing the fragments to adopt equilibrium geometries (using the same method previously described for geometry optimization). Basis set superposition errors (BSSEs) were calculated through the use of ghost atoms with no nuclear charge and no electrons to contribute to the molecule (using the molecular fragments method).

Reaction of [(dmpe)₂MnH(=GePh₂)] (1a) with H₂ to afford mixtures containing 1a, H₂, and [(dmpe)₂MnH₂(GeHPh₂)] (2a). Approx. 10 mg of [(dmpe)₂MnH(=GePh₂)] (**1a**) was dissolved in approx. 0.6 mL of C₆D₆ or *d*₈-toluene, and the solution placed in a J-young NMR tube. The mixture was freeze/pump/thawed three times, and placed under 1 atm of H₂ at –95 °C, sealed, and warmed to room temperature. This reaction was monitored over time *in situ* by NMR spectroscopy and had reached equilibrium within 3 days with 87% conversion to **2a**, at which time the solution had turned light orange. ¹H NMR (C₆D₆, 600 MHz, 298 K): δ 7.97 (d of d, 4H, ³J_{H,H} 7.9 Hz, ⁴J_{H,H} 1.4 Hz, *o*-Ph), 7.22 (t, 4H, ³J_{H,H} 7.4 Hz, *m*-Ph), 7.11 (t of t, 2H, ³J_{H,H} 7.3 Hz, ⁴J_{H,H} 1.4 Hz, *p*-Ph), 5.90 (m, 1H, GeH), 1.32 (m, 8H, PCH₂), 1.18 (br. s, 24H, PCH₃), –11.09 (br. m, 2H, MnH). ¹H NMR (*d*₈-toluene, 500 MHz, 298 K): δ 7.85 (d of d, 4H, ³J_{H,H} 6.5 Hz, ⁴J_{H,H} 1.3 Hz, *o*-Ph), 7.14 (t, 4H, ³J_{H,H} 7.3 Hz, *m*-Ph), 7.05 (t of t, 2H, ³J_{H,H} 7.3 Hz, ⁴J_{H,H} 1.9 Hz, *p*-Ph), 5.78 (m, 1H, GeH), 1.30 (m, 8H, PCH₂), 1.15 (br. s, 24H, PCH₃), –11.13 (br. m, 2H, MnH). ¹³C{¹H} NMR (*d*₈-toluene, 126 MHz, 298 K): δ 155.21 (s, *i*-Ph), 135.81 (s, *o*-Ph), 127.40 (s, *m*-Ph), 126.07 (s, *p*-Ph), 32.70 (m, PCH₂), 25.60 (m, PCH₃). ³¹P{¹H} NMR (*d*₈-toluene, 202 MHz, 298 K): δ 76.18 (s). *transHGe-2a*: ¹H NMR (*d*₈-toluene, 500 MHz, 176 K): δ 8.05 (d, 4H, ³J_{H,H} 7.1 Hz, *o*-Ph), 7.27 (t, 4H, ³J_{H,H} 7.2 Hz, *m*-Ph), 7.14 (t, 2H, ³J_{H,H} 7.2 Hz, *p*-Ph), 6.05 (d, 1H, ²J_{H,H} 15.8 Hz, GeH), 1.46, 1.21 (2 \times br. s, 4H,



PCH_2), 1.24, 0.96 ($2 \times s$, 12H, PCH_3), -10.53 (m, 1H, $MnHGe$), -11.19 (quin, 1H, $^2J_{H,P}$ 57.9 Hz, MnH). $^{13}C\{^1H\}$ NMR (*d*₈-toluene, 126 MHz, 176 K): δ 154.76 (s, *i*-Ph), 135.24 (s, *o*-Ph), 127.51 (s, *m*-Ph), 126.20 (s, *p*-Ph), 31.43 (m, PCH_2), 28.66, 21.51 ($2 \times s$, PCH_3). $^{31}P\{^1H\}$ NMR (*d*₈-toluene, 202 MHz, 176 K): δ 78.14 (s). **Isomers(s) of 2a with a disphenoidal arrangement of the phosphine donors (selected data):** 1H NMR (*d*₈-toluene, 500 MHz, 176 K): δ 8.32 (d, 2H, $^3J_{H,H}$ 6.9 Hz, *o*-Ph), 7.99 (d, 2H, $^3J_{H,H}$ 7.0 Hz, *o*-Ph), 7.42 (t, 2H, $^3J_{H,H}$ 7.1 Hz, *m*-Ph), 7.24 (t, 2H, $^3J_{H,H}$ 7.3 Hz, *m*-Ph), 5.49 (m, 1H, GeH), 1.52, 1.26, 1.00, 0.81, 0.57 ($5 \times s$, 3H, PCH_3), 1.39 (d, 3H, $^2J_{H,P}$ 5.6 Hz, PCH_3), 0.74 (d, 3H, $^2J_{H,P}$ 4.6 Hz, PCH_3), 0.72 (d, 3H, $^2J_{H,P}$ 4.0 Hz, PCH_3), -13.29 (br. s, 2H, MnH). $^{13}C\{^1H\}$ NMR (*d*₈-toluene, 126 MHz, 176 K): δ 156.67 (s, *i*-Ph), 136.67 (s, *o*-Ph), 127.09 (s, *m*-Ph), 29.94 (d, $J_{C,P}$ 20.2 Hz, PCH_3), 28.17, 25.10, 23.04, 21.18 ($4 \times s$, PCH_3), 27.57 (d, $J_{C,P}$ 18.5 Hz, PCH_3), 21.90 (d, $J_{C,P}$ 10.0 Hz, PCH_3), 19.51 (d, $J_{C,P}$ 15.5 Hz, PCH_3). $^{31}P\{^1H\}$ NMR (*d*₈-toluene, 202 MHz, 176 K): δ 76.11, 73.42 ($2 \times s$, 1P), 71.22 (s, 2P).

Reaction of [(dmpe)₂MnH(=GeEt₂)] (1b) with H₂ to afford mixtures containing 1b, H₂, and [(dmpe)₂MnH₂(GeHEt₂)] (2b). This was done in an analogous fashion to the reaction between 1a and H₂, using [(dmpe)₂MnH(=GeEt₂)] (1b) in place of 1a, and resulting in 73% conversion to 2b after reaching equilibrium (after 2 days), at which time the solution had turned yellow. 1H NMR (C₆D₆, 600 MHz, 298 K): δ 4.28 (s, 1H, GeH), 1.61 (t, 6H, $^3J_{H,H}$ 7.8 Hz, CH_2CH_3), 1.35 (m, 8H, PCH_2), 1.23 (s, 24H, PCH_3), 1.09, 1.00 ($2 \times m$, 2H, CH_2CH_3), -11.93 (m, 2H, MnH). 1H NMR (*d*₈-toluene, 500 MHz, 298 K): δ 4.15 (s, 1H, GeH), 1.41 (t, 6H, $^3J_{H,H}$ 7.8 Hz, CH_2CH_3), 1.33 (m, 8H, PCH_2), 1.21 (s, 24H, PCH_3), 0.99, 0.91 ($2 \times m$, 2H, CH_2CH_3), -12.00 (m, 2H, MnH). $^{13}C\{^1H\}$ NMR (*d*₈-toluene, 126 MHz, 298 K): δ 33.54 (m, PCH_2), 25.48 (s, PCH_3), 16.10 (s, CH_2CH_3), 14.59 (s, CH_2CH_3). $^{31}P\{^1H\}$ NMR (*d*₈-toluene, 202 MHz, 298 K): δ 75.53 (s). **transHGe-2b:** 1H NMR (*d*₈-toluene, 500 MHz, 176 K): δ 4.55 (s, GeH , 1H), 1.73 (m, 6H, CH_2CH_3), 1.52, 1.24 ($2 \times$ br. s, 4H, PCH_2), 1.32, 1.10 ($2 \times s$, PCH_3 , 12H), 1.22, 1.01 ($2 \times CH_2CH_3$), $\dagger\dagger$ -11.01 (m, 1H, $MnHGe$), -11.28 (quin, 1H, $^2J_{H,P}$ 56.0 Hz, MnH). $^{13}C\{^1H\}$ NMR (*d*₈-toluene, 126 MHz, 176 K): δ 32.73 (m, PCH_2), 27.52 (m, PCH_3), 22.37 (s, PCH_3), 15.23 (s, CH_2CH_3), 14.28 (s, CH_2CH_3). $^{31}P\{^1H\}$ NMR (*d*₈-toluene, 202 MHz, 176 K): δ 76.49 (s). **Isomers(s) of 2b with a disphenoidal arrangement of the phosphine donors (selected data):** 1H NMR (*d*₈-toluene, 500 MHz, 176 K): δ 3.86 (s, 1H, GeH), 2.08 (m, 3H, CH_2CH_3), 1.91, 1.28, 1.12 ($3 \times PCH_3$), $\dagger\dagger$ 1.37, 0.99, 0.95, 0.94 0.76 ($5 \times s$, 3H, PCH_3), 1.36 (CH_2CH_3), $\dagger\dagger$ -13.85 (br. s, 2H, MnH). $^{13}C\{^1H\}$ NMR (*d*₈-toluene, 126 MHz, 176 K): δ 25.03 (d, $J_{C,P}$ 12.8 Hz, PCH_3), 22.69 (d, $J_{C,P}$ 11.8 Hz, PCH_3), 22.66 (m, PCH_3), 16.89 (s, CH_2CH_3), 16.06 (s, PCH_3). $^{31}P\{^1H\}$ NMR (*d*₈-toluene, 202 MHz, 176 K): δ 74.65 (s, 2P), 72.68, 71.97 ($2 \times s$, 1P).

Reactions of [(dmpe)₂MnH(=GeR₂)] (R = Ph: 1a, R = Et: 1b) with D₂ to afford mixtures containing 1a or 1b, D₂, and

[(dmpe)₂MnD₂(GeHR₂)] (R = Ph: *d*₂-2a, R = Et: *d*₂-2b). These reactions were conducted in an analogous fashion to those described above for reactions of 1a–b with H₂ (in C₆D₆ or *d*₈-toluene), but using D₂ in place of H₂. To monitor deuterium scrambling in 2a, the reaction (in C₆D₆) was heated in the J-young tube at 60 °C and periodically analysed by NMR spectroscopy at room temperature. 1H and $^{31}P\{^1H\}$ NMR spectra at 298 K in C₆D₆ of 2a–b mirror those of 1a–b, with the exception that the MnH 1H NMR environment is not present and the GeH 1H NMR signal shifted slightly to 5.87 (*d*₂-2a) or 4.24 (*d*₂-2b) ppm. [(dmpe)₂MnD₂(HGePh₂)] (*d*₂-2a): 2H NMR (C₆D₆, 77 MHz, 298 K): δ -11.28 (app. t, $^2J_{D,P}$ 5.0 Hz, MnD). [(dmpe)₂MnD₂(HGeEt₂)] (*d*₂-2b): 2H NMR (C₆D₆, 77 MHz, 298 K): δ -12.16 (quin, $^2J_{D,P}$ 4.7 Hz, MnD).

X-ray quality crystals of [(dmpe)₂MnH(=GeEt₂)] (1b) and transHGe-[(dmpe)₂MnH(HGeHEt₂)] (transHGe-2b). 11.7 mg (0.02 mmol) of [(dmpe)₂MnH(=GeEt₂)] (1b) was dissolved in 0.35 mL of toluene, and the solution was placed in a 25 mL Schlenk flask, freeze/pump/thawed three times, placed under 1 atm of H₂ at -78 °C, sealed, and warmed to room temperature. The reaction mixture was then stirred for 2 days, after which the solvent was removed *in vacuo*, ~ 0.5 mL of hexanes was added, and the solution was placed under 1 atm of H₂ at -78 °C and sealed. Maintaining the solution at -78 °C for a few hours afforded large yellow X-ray quality crystals containing a mixture of 1b and transHGe-2b (due to disorder between two germyl groups and a germylene group in a 0.402 (3):0.056(3):0.542(3) ratio).

[(dmpe)₂Mn(GeHPh₂)(CN^tBu)] (3a). (a) 75.2 mg (0.13 mmol) of [(dmpe)₂MnH(=GePh₂)] (1a) was dissolved in 10 mL of benzene and placed in a 50 mL storage flask. 21.4 mg (0.26 mmol) of *tert*-butyl isonitrile was added and the reaction mixture was stirred for 1.5 hours at room temperature in the dark. The solvent was removed *in vacuo*, and the resulting yellow solid was dried *in vacuo* for 1 hour and washed with 4 mL of hexanes. Recrystallization of the residue (which did not dissolve in hexanes) at -30 °C from a solution in toluene layered with the hexanes that had been used to wash the crude material afforded 36.0 mg (0.05 mmol, 42%) of *cis*-3a as X-ray quality yellow crystals. The reaction of 1a with CN^tBu affords 3a in near quantitative spectroscopic yield (as a mixture of *cis* and *trans* isomers), so the low yield is due to losses during crystallization. (b) 15.3 mg (0.03 mmol) of [(dmpe)₂MnH(=GePh₂)] (1a) and 4.4 mg (0.05 mmol) of *tert*-butyl isonitrile were dissolved in approx. 0.6 mL of C₆D₆, placed in a J-young tube, and the reaction mixture was monitored over time at room temperature by NMR spectroscopy. After 30 minutes, the reaction mixture contained *cis*-3a and *trans*-3a in a 3 : 1 ratio, which remained constant over 4 days. *cis*-3a: 1H NMR (C₆D₆, 600 MHz, 298 K): δ 8.20, 8.15 ($2 \times d$ of d, 2H, $^3J_{H,H}$ 7.6 Hz, $^4J_{H,H}$ 1.0 Hz, *o*-Ph), 7.25, 7.22 ($2 \times t$, 2H, $^3J_{H,H}$ 7.9 Hz, *m*-Ph), 7.12 (t, 1H, $^3J_{H,H}$ 7.6 Hz, *p*-Ph), 7.08 (t, 1H, $^3J_{H,H}$ 7.4 Hz, *p*-Ph), 5.45 (t of d, 1H, $^3J_{H,P}$ 8.6 and 5.2 Hz, GeH), 1.80, 1.62 ($2 \times m$, 1H, PCH_2), 1.71 (d, 3H, $^2J_{H,P}$ 6.7 Hz, PCH_3), 1.69 (d, 3H, $^2J_{H,P}$ 6.9 Hz, PCH_3), 0.94–1.49 (m, 6H, PCH_2), 1.34, 1.16 ($2 \times d$, 3H, $^2J_{H,P}$ 6.6 Hz, PCH_3), 1.20 (d, 3H, $^2J_{H,P}$ 5.9 Hz, PCH_3), 1.10 (d,

$\dagger\dagger$ This NMR environment was located using 2D NMR spectroscopy, and thus no integration and/or environment splitting information is provided.



3H, $^2J_{\text{H,P}}$ 5.8 Hz, PCH_3), 1.03 (s, 9H, $\text{C}(\text{CH}_3)_3$), 0.97 (d, 3H, $^2J_{\text{H,P}}$ 4.6 Hz, PCH_3), 0.82 (d, 3H, $^2J_{\text{H,P}}$ 4.8 Hz, PCH_3). $^{13}\text{C}\{^1\text{H}\}$ NMR (C_6D_6 , 151 MHz, 298 K): δ 158.29 (d, $^3J_{\text{C,P}}$ 2.6 Hz, *i*-Ph), 157.74 (d, $^3J_{\text{C,P}}$ 3.4 Hz, *i*-Ph), 137.65, 137.47 (2 \times s, *o*-Ph), 127.23, 127.10 (2 \times s, *m*-Ph), 125.23, 125.20 (2 \times s, *p*-Ph), 54.94 (s, CMe_3), 34.62 (app. t of d, $J_{\text{C,P}}$ 20.7 and 5.5 Hz, PCH_2), 33.64 (app. t of d, $J_{\text{C,P}}$ 23.3 and 7.5 Hz, PCH_2), 33.13 (app. t, $J_{\text{C,P}}$ 20.4 Hz, PCH_2), 31.46 (s, $\text{C}(\text{CH}_3)_3$), 30.62 (app. t, $J_{\text{C,P}}$ 19 Hz, PCH_2), 24.31 (d of d, $J_{\text{C,P}}$ 14.1 and 5.2 Hz, PCH_3), 23.92 (d, $J_{\text{C,P}}$ 12.4 Hz, PCH_3), 23.43 (d of d, $J_{\text{C,P}}$ 16.0 and 5.8 Hz, PCH_3), 23.04 (d, $J_{\text{C,P}}$ 8.0 Hz, PCH_3), 22.40 (d of d, $J_{\text{C,P}}$ 17.9 and 6.0 Hz, PCH_3), 21.73 (m, PCH_3), 21.01 (d of m, $J_{\text{C,P}}$ 20.5 Hz, PCH_3). $^{31}\text{P}\{^1\text{H}\}$ NMR (C_6D_6 , 243 MHz, 298 K): δ 75.78, 56.99 (2 \times s, 1P), 70.53 (s, 2P). **trans-3a**: ^1H NMR (C_6D_6 , 500 MHz, 298 K): δ 8.00 (d, 4H, $^3J_{\text{H,H}}$ 7.1 Hz, *o*-Ph), 7.19 (m, *m*-Ph), 5.12 (quin., 1H, $^3J_{\text{H,P}}$ 7.7 Hz, GeH), 1.85, 1.44 (2 \times m, 4H, PCH_2), 1.40, 1.18 (2 \times s, 12H, PCH_3), 0.98 (s, 9H, $\text{C}(\text{CH}_3)_3$). $^{13}\text{C}\{^1\text{H}\}$ NMR (C_6D_6 , 126 MHz, 298 K): δ 158.83 (s, *i*-Ph), 137.10 (s, *o*-Ph), 127.38 (s, *m*-Ph), 125.36 (s, *p*-Ph), 54.55 (s, CMe_3), 32.52 (m, PCH_2), 31.36 (s, $\text{C}(\text{CH}_3)_3$), 21.72 (m, PCH_3). $^{31}\text{P}\{^1\text{H}\}$ NMR (C_6D_6 , 202 MHz, 298 K): δ 72.71 (s). Anal. found (calcd): C, 52.31 (52.28); H, 8.00 (7.87); N, 2.10 (2.08).

Monitoring of conversion for reactions of 1a with isonitriles to form [(dmpe) $_2$ Mn(GeHPh $_2$)(CNR)] (3b: R = *o*-xylyl, 3c: R = *n*-Bu). [(dmpe) $_2$ MnH(=GePh $_2$)] (1a; for 3b 11.6 mg/0.02 mmol, and for 3c 13.3 mg/0.02 mmol) and free isonitrile (for 3b 5.2 mg/0.04 mmol of *o*-xylyl isonitrile, and for 3c 7.0 mg/0.08 mmol of *n*-butyl isonitrile) were dissolved in approx. 0.6 mL of C_6D_6 , placed in a J-young tube, and the reaction mixtures were monitored over time at room temperature by NMR spectroscopy. Both reactions were complete after 1 hour. **cis-3b: ^1H NMR (C_6D_6 , 600 MHz, 298 K): δ 8.07 (d of m, 2H, $^3J_{\text{H,H}}$ 7.2 Hz, *o*-Ph), 8.03 (d of d, 2H, $^3J_{\text{H,H}}$ 7.8 Hz, $^4J_{\text{H,H}}$ 1.2 Hz, *o*-Ph), 7.13 (t, 2H, $^3J_{\text{H,H}}$ 7.4 Hz, *m*-Ph), 7.07 (m, 2H, *p*-Ph), 7.06 (m, 2H, *m*-Ph), 6.90 (d, 2H, $^3J_{\text{H,H}}$ 7.5 Hz, xylyl-*m*), 6.80 (t, 1H, $^3J_{\text{H,H}}$ 7.5 Hz, xylyl-*p*), 5.48 (q, 1H, $^3J_{\text{H,P}}$ 6.6 Hz, GeH), 2.10 (s, 6H, xylyl- CH_3), 1.72 (d, 3H, $^2J_{\text{H,P}}$ 7.0 Hz, PCH_3), 1.63 (d, 3H, $^2J_{\text{H,P}}$ 6.8 Hz, PCH_3), 1.47–1.61 (m, 2H, PCH_2), 1.51, 1.13 (2 \times d, 3H, $^2J_{\text{H,P}}$ 6.2 Hz, PCH_3), 1.04–1.40 (m, 5H, PCH_2), 1.19 (d, 3H, $^2J_{\text{H,P}}$ 5.9 Hz, PCH_3), 0.98 (d, 3H, $^2J_{\text{H,P}}$ 6.1 Hz, PCH_3), 0.90, 0.80 (2 \times d, 3H, $^2J_{\text{H,P}}$ 4.8 Hz, PCH_3), 0.88 (m, 1H, PCH_2). $^{13}\text{C}\{^1\text{H}\}$ NMR (C_6D_6 , 151 MHz, 298 K): δ 156.22 (s, *i*-Ph), 155.39 (d, $^3J_{\text{C,P}}$ 4.0 Hz, *i*-Ph), 137.78, 137.19 (2 \times s, *o*-Ph), 133.69 (s, xylyl-*i*), 133.11 (s, xylyl-*o*), 128.16 (xylyl-*m*), 127.22, 127.10 (2 \times s, *m*-Ph), 125.41, 125.36 (2 \times s, *p*-Ph), 122.62 (s, xylyl-*p*), 33.81 (app. t, $J_{\text{C,P}}$ 19.9 Hz, PCH_2), 33.17 (m, PCH_2), 31.86 (app. t, $J_{\text{C,P}}$ 20.1 Hz, PCH_2), 23.68 (d of m, $J_{\text{C,P}}$ 16.0 Hz, PCH_3), 22.50, 21.74, 21.05 (3 \times m, PCH_3), 20.72 (s, xylyl- CH_3). $^{31}\text{P}\{^1\text{H}\}$ NMR (C_6D_6 , 243 MHz, 298 K): δ 70.57 (s, 2P), 67.94, 53.44 (2 \times s, 1P). **trans-3b**: ^1H NMR (C_6D_6 , 600 MHz, 298 K): δ 7.95 (d of d, 4H, $^3J_{\text{H,H}}$ 7.7 Hz, $^4J_{\text{H,H}}$ 1.2 Hz, *o*-Ph), 7.18 (t, 4H, $^3J_{\text{H,H}}$ 7.3 Hz, *m*-Ph), 7.07 (m, 2H, *p*-Ph), 6.83 (d, 2H, $^3J_{\text{H,H}}$ 7.5 Hz, xylyl-*m*), 6.69 (t, 1H, $^3J_{\text{H,H}}$ 7.5 Hz, xylyl-*p*), 5.27 (quin., 1H, $^3J_{\text{H,P}}$ 7.3 Hz, GeH), 2.24 (s, 6H, xylyl- CH_3), 1.71, 1.52 (2 \times m, 4H, PCH_2), 1.41, 1.21 (2 \times s, 12H, PCH_3). $^{13}\text{C}\{^1\text{H}\}$ NMR (C_6D_6 , 151 MHz, 298 K): δ 157.67 (s, *i*-Ph), 137.32 (s, *o*-Ph), 133.81 (s, xylyl-*i*), 132.11 (s, xylyl-*o*), 128.68 (s, xylyl-*m*), 127.50 (s, *m*-Ph), 125.60**

(s, *p*-Ph), 122.25 (s, xylyl-*p*), 32.86 (m, PCH_2), 22.49, 21.91 (2 \times m, PCH_3), 20.63 (s, xylyl- CH_3). $^{31}\text{P}\{^1\text{H}\}$ NMR (C_6D_6 , 243 MHz, 298 K): δ 70.57 (s). **cis-3c**: ^1H NMR (C_6D_6 , 600 MHz, 298 K): δ 8.21, 8.13 (2 \times d, 2H, $^3J_{\text{H,H}}$ 7.8 Hz, *o*-Ph), 7.27, 7.22 (2 \times t, 2H, $^3J_{\text{H,H}}$ 7.5 Hz, *m*-Ph), 7.15 (t, 1H, $^3J_{\text{H,H}}$ 7.5 Hz, *p*-Ph), 7.11 (t, 1H, $^3J_{\text{H,H}}$ 7.3 Hz, *p*-Ph), 5.46 (app. t of d, 1H, $^3J_{\text{H,P}}$ 8.6 and 4.7 Hz, GeH), 3.16 (m, 2H, $\text{CH}_2\text{CH}_2\text{CH}_2\text{CH}_3$), 1.75, 1.61, 1.40 (3 \times m, 1H, PCH_2), 1.64, 1.18 (2 \times d, 3H, $^2J_{\text{H,P}}$ 6.2 Hz, PCH_3), 1.62 (d, 3H, $^2J_{\text{H,P}}$ 6.5 Hz, PCH_3), 1.39, 1.14, 1.06 (3 \times d, 3H, $^2J_{\text{H,P}}$ 6.0 Hz, PCH_3), 1.21 (m, 2H, $\text{CH}_2\text{CH}_2\text{CH}_2\text{CH}_3$), 1.19 (m, 2H, $\text{CH}_2\text{CH}_2\text{CH}_2\text{CH}_3$), 1.07–1.12 (m, 3H, PCH_2), 0.92–1.05 (m, 2H, PCH_2), 0.95 (d, 3H, $^2J_{\text{H,P}}$ 4.7 Hz, PCH_3), 0.81 (d, 3H, $^2J_{\text{H,P}}$ 4.9 Hz, PCH_3), 0.79 (t, 3H, $^3J_{\text{H,H}}$ 7.1 Hz, $\text{CH}_2\text{CH}_2\text{CH}_2\text{CH}_3$). $^{13}\text{C}\{^1\text{H}\}$ NMR (C_6D_6 , 151 MHz, 298 K): δ 157.61, 157.41 (2 \times s, *i*-Ph), 137.63, 137.28 (2 \times s, *o*-Ph), 127.20, 127.13 (2 \times s, *m*-Ph), 125.30, 125.27 (2 \times s, *p*-Ph), 45.12 (s, $\text{CH}_2\text{CH}_2\text{CH}_2\text{CH}_3$), 34.22, 33.41 (2 \times m, PCH_2), 33.08 (s, $\text{CH}_2\text{CH}_2\text{CH}_2\text{CH}_3$), 30.48 (app. t, $J_{\text{C,P}}$ 19.3 Hz, PCH_2), 24.47, 23.01, 22.85, 21.34, 21.11, 20.95 (6 \times m, PCH_3), 23.53 (d, $J_{\text{C,P}}$ 13.2 Hz, PCH_3), 22.38 (d of d, $J_{\text{C,P}}$ 20.3 and 5.6 Hz, PCH_3), 20.40 (s, $\text{CH}_2\text{CH}_2\text{CH}_2\text{CH}_3$), 13.76 (s, $\text{CH}_2\text{CH}_2\text{CH}_2\text{CH}_3$). $^{31}\text{P}\{^1\text{H}\}$ NMR (C_6D_6 , 243 MHz, 298 K): δ 76.11, 53.33 (2 \times s, 1P), 71.59 (s, 2P). **trans-3c (selected)**: ^1H NMR (C_6D_6 , 600 MHz, 298 K): δ 7.96 (d, 4H, $^3J_{\text{H,H}}$ 7.1 Hz, *o*-Ph), 5.06 (quin., 1H, $^3J_{\text{H,P}}$ 15.5 Hz, GeH), 1.81, 1.43 (2 \times m, 4H, PCH_2), 1.36, 1.16 (2 \times s, 12H, PCH_3). $^{13}\text{C}\{^1\text{H}\}$ NMR (C_6D_6 , 151 MHz, 298 K): δ 137.01 (s, *o*), 127.42, 125.45 (2 \times s, *m* and *p*), 32.26 (m, PCH_2), 22.97, 21.30 (2 \times m, PCH_3). $^{31}\text{P}\{^1\text{H}\}$ NMR (C_6D_6 , 243 MHz, 298 K): δ 73.77 (s).

X-ray quality crystals of cis-[(dmpe) $_2$ Mn(GeHPh $_2$)(CNXyl)] (3b) and [(dmpe) $_2$ MnH(CNXyl)] (4). The reaction of 1a with *o*-xylyl isonitrile was allowed to proceed to completion as described above, at which point it was heated overnight at 100 $^\circ\text{C}$ to afford a mixture containing **cis-3b**, **trans-3b**, and 4 in a 24 : 3 : 73 ratio. The solvent was then removed *in vacuo*, the resulting solid was extracted with hexanes, and the mother liquors were stored at $-30\text{ }^\circ\text{C}$ to afford X-ray quality yellow crystals of 4. The remaining solid (which did not dissolve in hexanes) was dissolved in minimal toluene, and that solution was stored at $-30\text{ }^\circ\text{C}$ to afford yellow crystals from which an X-ray structure of **cis-3b** was obtained.

X-ray quality crystals of trans-[(dmpe) $_2$ Mn(GeHPh $_2$)(CN n Bu)] (3c). 47.7 mg (0.08 mmol) of [(dmpe) $_2$ MnH(=GePh $_2$)] (1a) was dissolved in 5 mL of benzene, and the solution was transferred to a 50 mL storage flask. 25.1 mg (0.30 mmol) of *n*-butyl isonitrile was added, and the reaction was stirred for 1 hour at room temperature. Removal of the solvent *in vacuo* afforded an orange oil which was dried *in vacuo* for 1 hour at room temperature. The oil was extracted with 1.5 mL of hexanes to afford an orange solution which was stored at $-30\text{ }^\circ\text{C}$ to afford yellow crystals from which an X-ray structure of **trans-3c** was obtained. Recrystallization of the residue (which did not dissolve in hexanes) at $-30\text{ }^\circ\text{C}$ from toluene layered with hexanes afforded 4.7 mg (0.01 mmol) of **cis-3c**, in >95% purity (measured by NMR spectroscopy).

[(dmpe) $_2$ Mn(GeHPh $_2$)(N $_2$)] (5a). 50.1 mg (0.09 mmol) of [(dmpe) $_2$ MnH(=GePh $_2$)] (1a) was dissolved in 5 mL of benzene



and placed in a 100 mL storage flask. The mixture was freeze/pump/thawed three times, placed under 1 atm of N₂ at −95 °C, sealed, and warmed to room temperature. After stirring for 5 days at room temperature in the dark, the solvent was removed *in vacuo*. The resulting solid was recrystallized from a concentrated solution of toluene layered with a concentrated solution of hexanes at −30 °C to afford 28.4 mg (0.05 mmol, 54%) of **5a** as yellow crystals. X-ray quality crystals of *cis*-**5a** were obtained by recrystallization from a concentrated solution in toluene layered with hexanes at −30 °C. X-ray quality crystals of *trans*-**5a** were obtained by serendipitous N₂ addition to a reaction mixture formed from the combination of approx. 10 mg of **1a** with H₂ in *d*₈-toluene, followed by removal of the solvent *in vacuo* and recrystallization from toluene at −30 °C. NMR spectra were obtained under an atmosphere of N₂. **cis**-**5a**: $\nu(\text{N}\equiv\text{N})$: 2010 cm^{−1}, $\nu(\text{Ge-H})$: 1860 cm^{−1} (very broad). ¹H NMR (C₆D₆, 600 MHz, 298 K): δ 8.22, 8.11 (2 × d, 2H, ³J_{H,H} 7.0 Hz, *o*-Ph), 7.34, 7.24 (2 × t, 2H, ³J_{H,H} 7.4 Hz, *m*-Ph), 7.17 (t, ³J_{H,H} 7.7 Hz, *p*-Ph), $\ddagger\ddagger$ 7.12 (t, 1H, ³J_{H,H} 7.3 Hz, *p*-Ph), 5.40 (q, 1H, ³J_{H,P} 5.4 Hz, GeH), 0.70–1.74 (m, 8H, PCH₂), 1.48 (d, 6H, ²J_{H,P} 6.8 Hz, PCH₃), 1.29 (PCH₃), $\ddagger\ddagger$ 1.09 (d, 3H, ²J_{H,P} 6.1 Hz, PCH₃), 0.99 (d, 3H, ²J_{H,P} 6.5 Hz, PCH₃), 0.93 (d, 3H, ²J_{H,P} 5.9 Hz, PCH₃), 0.85 (d, 3H, ²J_{H,P} 5.1 Hz, PCH₃), 0.53 (d, 3H, ²J_{H,P} 5.3 Hz, PCH₃). ¹³C{¹H} NMR (C₆D₆, 151 MHz, 298 K): δ 154.87, 153.61 (2 × s, *i*-Ph), 137.80, 137.22 (2 × s, *o*-Ph), 127.49, 127.34 (2 × s, *m*-Ph), 125.84 (s, *p*-Ph), 125.73 or 125.68 (s, *p*-Ph), §§ 33.18, 29.30 (2 × m, PCH₂), 32.53 (app. t, J_{C,P} 20.8 Hz, PCH₂), 23.09, 21.90, 21.80, 16.52 (4 × m, PCH₃), 22.64 (d of d, J_{C,P} 18.5 and 5.8 Hz, PCH₃), 19.87 (d, J_{C,P} 16.8 Hz, PCH₃), 17.45 (d, J_{C,P} 18.7 Hz, PCH₃), 15.31 (d of d, J_{C,P} 17.3 and 4.8 Hz, PCH₃). ³¹P{¹H} NMR (C₆D₆, 243 MHz, 298 K): δ 71.98, 69.33, 68.72, 58.71 (4 × s, 1P). ³¹P{¹H} NMR (*d*₈-toluene, 202 MHz, 223 K): δ 72.47, 70.27, 68.91, 58.75 (4 × s, 1P). ⁵⁵Mn{¹H} NMR (*d*₈-toluene, 124 MHz, 298 K): δ −718 (br. s). ⁵⁵Mn{¹H} NMR (*d*₈-toluene, 124 MHz, 223 K): δ −812 (br. s). ⁵⁵Mn{¹H} NMR (*d*₈-toluene, 124 MHz, 370 K): δ −601 (br. s). *trans*-**5a**: $\nu(\text{N}\equiv\text{N})$: 1973 cm^{−1}, $\nu(\text{Ge-H})$: 1860 cm^{−1} (very broad). ¹H NMR (C₆D₆, 600 MHz, 298 K): δ 7.81 (d, 4H, ³J_{H,H} 7.0 Hz, *o*-Ph), 7.12 (t, 4H, ³J_{H,H} 7.3 Hz, *m*-Ph), 7.04 (t, 2H, ³J_{H,H} 7.2 Hz, *p*-Ph), 4.74 (quin., 1H, ³J_{H,P} 7.7 Hz, GeH), 1.80, 1.38 (2 × m, 4H, PCH₂), 1.29, 1.16 (2 × s, 12H, PCH₃). ¹³C{¹H} NMR (C₆D₆, 151 MHz, 298 K): δ 156.81 (s, *i*-Ph), 136.69 (s, *o*-Ph), 127.49 (s, *m*-Ph), 125.73 or 125.68 (s, *p*-Ph), §§ 31.35 (m, PCH₂), 20.28, 16.48 (2 × m, PCH₃). ³¹P{¹H} NMR (C₆D₆, 243 MHz, 298 K): δ 70.63 (br. s). ³¹P{¹H} NMR (*d*₈-toluene, 202 MHz, 223 K): δ 71.37 (s). ³¹P{¹H} NMR (*d*₈-toluene, 202 MHz, 370 K): δ 70.2 (broad multiplet with nearly indiscernible coupling due to quadrupolar collapse). ⁵⁵Mn{¹H} NMR (*d*₈-toluene, 124 MHz, 298 K): δ −845 (br. s). ⁵⁵Mn{¹H} NMR (*d*₈-toluene, 124 MHz, 223 K): δ −991 (br. s). ⁵⁵Mn{¹H} NMR (*d*₈-toluene, 124 MHz, 370 K): δ −730 (br. s). Anal. found (calcd): C, 47.25 (47.17); H, 7.14 (7.09); N, 4.42 (4.58).

$\ddagger\ddagger$ This NMR signal could not be integrated because of overlap with a residual solvent signal.

§§ The *p*-Ph ¹³C NMR signals for the *cis* and *trans* isomers are too close in chemical shift to determine which signals correspond to which isomer.

Repetition of EA after 2.7 years sealed under argon at −30 °C: Anal. found (calcd): C, 46.96 (47.17); H, 7.20 (7.09); N, 3.84 (4.58).

[(dmpe)₂Mn(GeHEt₂)(N₂)] (**5b**). 106.5 mg (0.22 mmol) of [(dmpe)₂MnH(=GeEt₂)] (**1b**) was dissolved in 10 mL of benzene and transferred to a 100 mL storage flask. The mixture was freeze/pump/thawed three times, placed under 1 atm of N₂ at −95 °C, sealed, and warmed to room temperature. After stirring for 3 days at room temperature in the dark, the solvent was removed *in vacuo*. The resulting solid was recrystallized using 5 mL of hexanes at −30 °C to afford 65.3 mg (0.13 mmol, 58%) of *cis*-**5b** as yellow crystals. X-ray quality crystals of *trans*-**5b** were obtained by heating a mixture of approx. 10 mg of **1b** under N₂ for 4 days at 60 °C in C₆D₆ (which resulted in *cis*–*trans* isomerization to a 22:78 ratio), followed by removal of the solvent *in vacuo* and recrystallization from a concentrated solution of hexanes at −30 °C. NMR spectra were obtained under an atmosphere of N₂. *cis*-**5b**: $\nu(\text{N}\equiv\text{N})$: 1989 cm^{−1}, $\nu(\text{Ge-H})$: 1823 cm^{−1}. ¹H NMR (C₆D₆, 600 MHz, 298 K): δ 3.65 (m, 1H, GeH), 1.83, 1.82 (2 × t, 3H, ³J_{H,H} 7.8 Hz, CH₂CH₃), 1.63 (m, 1H, PCH₂), 1.54 (d, 3H, ²J_{H,P} 7.1 Hz, PCH₃), 1.23–1.56 (m, 4H, PCH₂), 1.50, 1.33, 1.32, 1.27 (4 × m, 1H, CH₂CH₃), 1.47 (d, 3H, ²J_{H,P} 6.7 Hz, PCH₃), 1.14 (d, 3H, ²J_{H,P} 6.3 Hz, PCH₃), 1.12 (d, 3H, ²J_{H,P} 5.8 Hz, PCH₃), 1.06 (d, 3H, ²J_{H,P} 6.5 Hz, PCH₃), 1.03 (d, 3H, ²J_{H,P} 5.9 Hz, PCH₃), 0.97 (d, 3H, ²J_{H,P} 5.0 Hz, PCH₃), 0.70–0.94 (m, 3H, PCH₂), 0.58 (d, 3H, ²J_{H,P} 5.2 Hz, PCH₃). ¹³C{¹H} NMR (C₆D₆, 151 MHz, 298 K): δ 33.97 (m, PCH₂), 31.36 (app. t, J_{C,P} 19.7 Hz, PCH₂), 28.90 (d of d, J_{C,P} 23.5 and 16.4 Hz, PCH₂), 22.69 (app. d of t, J_{C,P} 13.1 and 2.7 Hz, PCH₃), 21.99 (d of d, J_{C,P} 13.1 and 5.0 Hz, PCH₃), 21.38 (d of m, J_{C,P} 12.2 Hz, PCH₃), 20.98, 16.45 (2 × m, PCH₃), 20.64 (d, J_{C,P} 13.9 Hz, PCH₃), 16.53, 16.02 (2 × s, CH₂CH₃), 15.78 (app. d of t, J_{C,P} 20.7 and 3.3 Hz, PCH₃), 15.32 (d of d, J_{C,P} 15.3 and 5.2 Hz, PCH₃), 12.47, 10.98 (2 × s, CH₂CH₃). ³¹P{¹H} NMR (C₆D₆, 243 MHz, 298 K): δ 75.51, 71.37, 65.43, 60.62 (4 × s, 1P). ³¹P{¹H} NMR (*d*₈-toluene, 202 MHz, 223 K): δ 75.98, 71.85, 65.68, 60.76 (4 × s, 1P). ⁵⁵Mn{¹H} NMR (*d*₈-toluene, 124 MHz, 298 K): δ −1011 (br. s). ⁵⁵Mn{¹H} NMR (*d*₈-toluene, 124 MHz, 223 K): δ −1070 (br. s). ⁵⁵Mn{¹H} NMR (*d*₈-toluene, 124 MHz, 370 K): δ −906 (br. s). *trans*-**5b**: $\nu(\text{N}\equiv\text{N})$: 1968 cm^{−1}, $\nu(\text{Ge-H})$: not detected. ¹H NMR (C₆D₆, 600 MHz, 298 K): δ 3.02 (m, 1H, GeH), 1.56, 1.34 (2 × m, 4H, PCH₂), 1.54 (t, 6H, ³J_{H,H} 7.7 Hz, CH₂CH₃), 1.35, 1.21 (2 × s, 12H, PCH₃), 0.66 (m, 4H, CH₂CH₃). ¹³C{¹H} NMR (C₆D₆, 151 MHz, 298 K): δ 31.55 (quin, J_{C,P} 11.7 Hz, PCH₂), 20.40, 16.53 (2 × m, PCH₃), 16.74 (s, CH₂CH₃), 15.38 (s, CH₂CH₃). ³¹P{¹H} NMR (C₆D₆, 243 MHz, 298 K): δ 72.51 (m). ³¹P{¹H} NMR (*d*₈-toluene, 202 MHz, 370 K): δ 71.79 (approx. 1:1:1:1:1:1 sextet, ¹J_{P,Mn} 274 Hz). ⁵⁵Mn{¹H} NMR (*d*₈-toluene, 124 MHz, 298 K): δ −1094 (quin, ¹J_{P,Mn} 275 Hz). ⁵⁵Mn{¹H} NMR (*d*₈-toluene, 124 MHz, 223 K): δ −1168 (s). ⁵⁵Mn{¹H} NMR (*d*₈-toluene, 124 MHz, 370 K): δ −982 (quin, ¹J_{P,Mn} 274 Hz). Anal. found (calcd): C, 37.33 (37.31); H, 8.49 (8.42); N, 5.48 (5.44). Repetition of EA after 1000 days sealed in argon at −30 °C Anal. found (calcd): C, 37.16 (37.31); H, 8.56 (8.42); N, 5.10 (5.44).

Monitoring of conversion and *cis* : *trans* ratios for reactions of **1a–**b** with N₂ to form [(dmpe)₂Mn(GeHR₂)(N₂)] (**5a**: R = Ph,**



5b: R = Et). Approx. 10 mg of $[(\text{dmpe})_2\text{MnH}(\text{=GeR}_2)]$ (**1a**: R = Ph, **1b**: R = Et) was dissolved in approx. 0.6 mL of C_6D_6 and the mixture was transferred to a J-young tube. The solutions were freeze/pump/thawed three times, placed under 1 atm of N_2 at -95°C , sealed, and warmed to room temperature. Conversion of **1a–b** to **5a–b**, along with *cis*:*trans* ratios of **5a–b**, were monitored by ^1H NMR spectroscopy at various intervals. In the case of the reaction involving **1b**, the reaction mixture was also heated at 60°C for various times and monitored by ^1H NMR spectroscopy.

$[(\text{dmpe})_2\text{Mn}(\text{SiHPh}_2)(\text{N}_2)]$ (**6**). Approx. 10 mg of a mixture containing $[(\text{dmpe})_2\text{MnH}(\text{=SiPh}_2)]$ and $[(\text{dmpe})_2\text{MnH}_2(\text{SiHPh}_2)]$ in a 6 : 1 ratio was dissolved in approx. 0.6 mL of C_6D_6 and the mixture was transferred to a J-young tube. The mixture was freeze/pump/thawed three times, placed under 1 atm of N_2 at -95°C , sealed, and warmed to room temperature. The resulting solution was analyzed by NMR spectroscopy *in situ* after sitting at room temperature for 2 hours, and contained $[(\text{dmpe})_2\text{MnH}_2(\text{SiHPh}_2)]$, *cis*- $[(\text{dmpe})_2\text{Mn}(\text{SiHPh}_2)(\text{N}_2)]$ (**cis-6**), and *trans*- $[(\text{dmpe})_2\text{Mn}(\text{SiHPh}_2)(\text{N}_2)]$ (**trans-6**) in a 1 : 5.7 : 2.3 ratio. X-ray quality crystals of **trans-6** were obtained by removing the solvent *in vacuo*, washing with 1 mL of hexanes, and recrystallization of the residue from 1 mL of toluene at -30°C . **cis-6** (selected): ^1H NMR (C_6D_6 , 600 MHz, 298 K): δ 8.24 (d of d, 2H, $^3J_{\text{H,H}}$ 7.7 Hz, $^4J_{\text{H,H}}$ 1.3 Hz, *o*-Ph), 8.15 (d of d, 2H, $^3J_{\text{H,H}}$ 8.0 Hz, $^4J_{\text{H,H}}$ 1.3 Hz, *o*-Ph), 7.32 (t, 2H, $^3J_{\text{H,H}}$ 7.7 Hz, *m*-Ph), 7.24 (t, 2H, $^3J_{\text{H,H}}$ 7.6 Hz, *m*-Ph), 7.16 (m, 2H, *p*-Ph), 5.53 (m w. ^{29}Si sat., 1H, $^1J_{\text{H,Si}}$ 141 Hz, SiH), 1.35, 1.30 (2 \times d, 3H, $J_{\text{H,P}}$ 6.6 Hz, PCH_3), 1.33 (d, 3H, $J_{\text{H,P}}$ 7.2 Hz, PCH_3), 1.17 (d, 3H, $J_{\text{H,P}}$ 5.6 Hz, PCH_3), 0.91 (d, 3H, $J_{\text{H,P}}$ 5.2 Hz, PCH_3), 0.90 (d, 3H, $J_{\text{H,P}}$ 4.7 Hz, PCH_3), 0.53 (d, 3H, $J_{\text{H,P}}$ 5.4 Hz, PCH_3). $^{13}\text{C}\{^1\text{H}\}$ NMR (C_6D_6 , 151 MHz, 298 K): δ 152.75, 151.83 (2 \times s, *i*-Ph), 137.25, 136.92 (2 \times s, *o*-Ph), 127.18 (s, *m*-Ph), 126.14 (s, *p*-Ph), 34.25 (t, $J_{\text{C,P}}$ 21.8 Hz, PCH_2), 32.90, 32.06 (2 \times m, PCH_2), 29.77 (d of d, $J_{\text{C,P}}$ 24.5 and 16.0 Hz, PCH_2), 24.71 (d of d, $J_{\text{C,P}}$ 13.2 and 4.8 Hz, PCH_3), 23.05 (d of d, $J_{\text{C,P}}$ 13.2 and 6.3 Hz, PCH_3), 22.57 (m, PCH_3), 19.75 (d, $J_{\text{C,P}}$ 19.7 Hz, PCH_3), 16.86 (d, $J_{\text{C,P}}$ 18.4 Hz, PCH_3), 15.95 (d of d, $J_{\text{C,P}}$ 18.5 and 5.4 Hz, PCH_3), 15.26 (d of d, $J_{\text{C,P}}$ 17.6 and 4.7 Hz, PCH_3). ^{29}Si NMR (data from ^{29}Si - ^1H HMBC in C_6D_6 , 119 MHz, 298 K): δ 36.0. $^{31}\text{P}\{^1\text{H}\}$ NMR (C_6D_6 , 243 MHz, 298 K): δ 71.78, 68.50, 64.12, 58.67 (4 \times s, 1P). $^{55}\text{Mn}\{^1\text{H}\}$ NMR (C_6D_6 , 124 MHz, 298 K): δ -973 (br. s). $^{55}\text{Mn}\{^1\text{H}\}$ NMR (C_6D_6 , 124 MHz, 360 K): δ -881 (br. s). **trans-6**: ^1H NMR (C_6D_6 , 600 MHz, 298 K): δ 7.78 (d of d, 4H, $^3J_{\text{H,H}}$ 7.8 Hz, $^4J_{\text{H,H}}$ 1.4 Hz, *o*-Ph), 7.11 (t, 4H, $^3J_{\text{H,H}}$ 7.3 Hz, *m*-Ph), 7.04 (t of t, 2H, $^3J_{\text{H,H}}$ 7.3 Hz, $^4J_{\text{H,H}}$ 1.4 Hz, *p*-Ph), 4.82 (quin. w. ^{29}Si sat., 1H, $^3J_{\text{H,P}}$ 8.6 Hz, $^1J_{\text{H,Si}}$ 140 Hz, SiH), 1.79, 1.35 (2 \times m, 4H, PCH_2), 1.27, 1.17 (2 \times s, 12H, PCH_3). $^{13}\text{C}\{^1\text{H}\}$ NMR (C_6D_6 , 151 MHz, 298 K): δ 154.10 (s, *i*-Ph), 136.39 (s, *o*-Ph), 127.31 (s, *m*-Ph), 126.01 (s, *p*-Ph), 31.31 (m, PCH_2), 20.55, 17.08 (2 \times m, PCH_3). ^{29}Si NMR (data from ^{29}Si - ^1H HMBC in C_6D_6 , 119 MHz, 298 K): δ 33.9. $^{31}\text{P}\{^1\text{H}\}$ NMR (C_6D_6 , 243 MHz, 298 K): δ 70.8 (m). $^{31}\text{P}\{^1\text{H}\}$ NMR (C_6D_6 , 202 MHz, 360 K): δ 70.39 (approx. 1 : 1 : 1 : 1 : 1 sextet, $^1J_{\text{P,Mn}}$ 269 Hz). $^{55}\text{Mn}\{^1\text{H}\}$ NMR (C_6D_6 , 124 MHz, 298 K): δ -1098 (quin, $^1J_{\text{P,Mn}}$ 270 Hz). $^{55}\text{Mn}\{^1\text{H}\}$ NMR (C_6D_6 , 124 MHz, 360 K): δ -1006 (quin, $^1J_{\text{P,Mn}}$ 270 Hz).

New spectroscopic data for previously reported $[(\text{dmpe})_2\text{MnH}(\text{=GeR}_2)]$ (1a**: R = Ph, **1b**: R = Et) and $[(\text{dmpe})_2\text{MnH}(\text{=SiPh}_2)]$.** Approximately 15 mg of $[(\text{dmpe})_2\text{MnH}(\text{=GePh}_2)]$ (**1a**), $[(\text{dmpe})_2\text{MnH}(\text{=GeEt}_2)]$ (**1b**), or an 8 : 1 mixture of $[(\text{dmpe})_2\text{MnH}(\text{=SiPh}_2)]$ and $[(\text{dmpe})_2\text{MnH}_2(\text{SiHPh}_2)]$ were dissolved in approx. 0.6 mL of (for **1a–b**) *d*₈-toluene or (for the silicon-containing species) C_6D_6 , and analyzed by NMR spectroscopy. **1a**: $^{55}\text{Mn}\{^1\text{H}\}$ NMR (*d*₈-toluene, 124 MHz, 298 K): δ -1176 (br. s). $^{55}\text{Mn}\{^1\text{H}\}$ NMR (*d*₈-toluene, 124 MHz, 370 K): δ -1107 (br. s). **1b**: $^{55}\text{Mn}\{^1\text{H}\}$ NMR (*d*₈-toluene, 124 MHz, 298 K): δ -1303 (br. s). $^{55}\text{Mn}\{^1\text{H}\}$ NMR (*d*₈-toluene, 124 MHz, 370 K): δ -1226 (br. s). $[(\text{dmpe})_2\text{MnH}(\text{=SiPh}_2)]$: $^{55}\text{Mn}\{^1\text{H}\}$ NMR (C_6D_6 , 124 MHz, 298 K): δ -548 (br. s).

Data availability

Data supporting this article is included in the ESI†. Crystallographic data for **trans-2a/1a**, **cis-3a**, **cis-3b**, **trans-3c**, **4**, **cis-5a**, **trans-5a**, **cis-5b**, **trans-5b**, and **6** has been deposited at the CCDC with deposition numbers 2447494–2447503,† respectively.

Conflicts of interest

There are no conflicts to declare.

Acknowledgements

D. J. H. E. thanks NSERC of Canada for a Discovery Grant and Dr Yuriy Mozharivskiy for access to his X-ray diffractometer. We are also grateful to Dr James Britten and Dr Gary Schrobilgen for helpful advice regarding X-ray crystal structures and analysis of NMR spectra involving coupling to quadrupolar nuclei, respectively, and Dr Novan Gray for assistance with high temperature NMR spectroscopy.

References

- J. Baumgartner and C. Marschner, *Rev. Inorg. Chem.*, 2014, **34**, 119–152.
- V. Y. Lee, *Eur. J. Inorg. Chem.*, 2022, e202200175.
- M. Ghosh, N. Sen and S. Khan, *ACS Omega*, 2022, **7**, 6449–6454.
- T. J. Hadlington, *Chem. Soc. Rev.*, 2024, **53**, 9738–9831.
- H. Hashimoto, T. Tsubota, T. Fukuda and H. Tobita, *Chem. Lett.*, 2009, **38**, 1196–1197.
- H. Sakaba, Y. Arai, K. Suganuma and E. Kwon, *Organometallics*, 2013, **32**, 5038–5046.
- T. Fukuda, H. Hashimoto and H. Tobita, *J. Organomet. Chem.*, 2017, **848**, 89–94.
- T. P. Dhungana, H. Hashimoto, M. Ray and H. Tobita, *Organometallics*, 2020, **39**, 4350–4361.



- 9 T. P. Dhungana, H. Hashimoto and H. Tobita, *Dalton Trans.*, 2017, **46**, 8167–8179.
- 10 M. Widemann, S. Jeggle, M. Auer, K. Eichele, H. Schubert, C. P. Sindlinger and L. Wesemann, *Chem. Sci.*, 2022, **13**, 3999–4009.
- 11 K. K. Pandey, M. Lein and G. Frenking, *J. Am. Chem. Soc.*, 2003, **125**, 1660–1668.
- 12 A. C. Filippou, U. Chakraborty and G. Schnakenburg, *Chem. – Eur. J.*, 2013, **19**, 5676–5686.
- 13 A. C. Filippou, N. Weidemann, A. I. Philippopoulos and G. Schnakenburg, *Angew. Chem., Int. Ed.*, 2006, **45**, 5987–5991.
- 14 H. Hashimoto, T. Fukuda, H. Tobita, M. Ray and S. Sakaki, *Angew. Chem., Int. Ed.*, 2012, **51**, 2930.
- 15 M. E. Fasulo and T. D. Tilley, *Chem. Commun.*, 2012, **48**, 7690–7692.
- 16 H. Hashimoto, T. Fukuda and H. Tobita, *New J. Chem.*, 2010, **34**, 1723–1730.
- 17 P. G. Hayes, R. Waterman, P. B. Glaser and T. D. Tilley, *Organometallics*, 2009, **28**, 5082–5089.
- 18 S. Bajo, E. Soto, M. Fernández-Buenestado, J. López-Serrano and J. Campos, *Nat. Commun.*, 2024, **15**, 9656.
- 19 K. E. Litz, K. Henderson, R. W. Gourley and M. M. B. Holl, *Organometallics*, 1995, **14**, 5008–5010.
- 20 S. Grumbine and T. D. Tilley, in *Progress in Organosilicon Chemistry*, ed. B. Marciniec and J. Chojnowski, Gordon and Breach, Amsterdam, 1995, pp. 133–146.
- 21 P. Gaspar and R. West, in *The Chemistry of Organic Silicon Compounds*, ed. Z. Rappoport and Y. Apeloig, John Wiley & Sons, Chichester, UK, 1998, vol. 2, ch. 43, pp. 2463–2568.
- 22 M. Okazaki, H. Tobita and H. Ogino, *Dalton Trans.*, 2003, 493–506.
- 23 R. Waterman, P. G. Hayes and T. D. Tilley, *Acc. Chem. Res.*, 2007, **40**, 712–719.
- 24 D. J. Cardin, B. Cetinkaya and M. F. Lappert, *Chem. Rev.*, 1972, **72**, 545–574.
- 25 D. J. Cardin, B. Cetinkaya, M. J. Doyle and M. F. Lappert, *Chem. Soc. Rev.*, 1973, **2**, 99–144.
- 26 T. Strassner, *Top. Organomet. Chem.*, 2004, 1–20.
- 27 G. S. Girolami, G. Wilkinson, M. Thornton-Pett and M. B. Hursthouse, *J. Am. Chem. Soc.*, 1983, **105**, 6752–6753.
- 28 G. S. Girolami, C. G. Howard, G. Wilkinson, H. M. Dawes, M. Thornton-Pett, M. Motevalli and M. B. Hursthouse, *J. Chem. Soc., Dalton Trans.*, 1985, 921–929.
- 29 J. S. Price, I. Vargas-Baca, D. J. H. Emslie and J. F. Britten, *Dalton Trans.*, 2023, **52**, 14880–14895.
- 30 J. S. Price, D. J. H. Emslie, I. Vargas-Baca and J. F. Britten, *Organometallics*, 2018, **37**, 3010–3023.
- 31 J. S. Price, D. J. H. Emslie and J. F. Britten, *Angew. Chem., Int. Ed.*, 2017, **56**, 6223–6227.
- 32 J. S. Price and D. J. H. Emslie, *Chem. Sci.*, 2019, **10**, 10853–10869.
- 33 J. S. Price, D. J. H. Emslie and B. Berno, *Organometallics*, 2019, **38**, 2347–2362.
- 34 J. S. Price and D. J. H. Emslie, *Organometallics*, 2020, **39**, 4618–4628.
- 35 H. M. Mobarok, R. McDonald, M. J. Ferguson and M. Cowie, *Inorg. Chem.*, 2012, **51**, 4020–4034.
- 36 K. A. Smart, E. Mothes-Martin, L. Vendier, R. N. Perutz, M. Grellier and S. Sabo-Etienne, *Organometallics*, 2015, **34**, 4158–4163.
- 37 P. M. Keil, S. Ezendu, A. Schulz, M. Kubisz, T. Szilvási and T. J. Hadlington, *J. Am. Chem. Soc.*, 2024, **146**, 23606–23615.
- 38 V. Y. Lee, R. Sakai, K. Takanashi, O. A. Gapurenko, R. M. Minyaev, H. Gornitzka and A. Sekiguchi, *Angew. Chem., Int. Ed.*, 2021, **60**, 3951–3955.
- 39 J. L. Vincent, S. Luo, B. L. Scott, R. Butcher, C. J. Unkefer, C. J. Burns, G. J. Kubas, A. Lledós, F. Maseras and J. Tomàs, *Organometallics*, 2003, **22**, 5307–5323.
- 40 R. Herrmann, T. Braun and S. Mebs, *Eur. J. Inorg. Chem.*, 2014, **2014**, 4826–4835.
- 41 A. Antiñolo, F. Carrillo-Hermosilla, A. Castel, M. Fajardo, J. Fernández-Baeza, M. Lanfranchi, A. Otero, M. A. Pellinghelli, G. Rima, J. Satgé and E. Villaseñor, *Organometallics*, 1998, **17**, 1523–1529.
- 42 N. Zhang, R. S. Sherbo, G. S. Bindra, D. Zhu and P. H. M. Budzelaar, *Organometallics*, 2017, **36**, 4123–4135.
- 43 J. Takaya and N. Iwasawa, *Eur. J. Inorg. Chem.*, 2018, **2018**, 5012–5018.
- 44 C. J. Laglera-Gándara, P. Ríos, F. J. Fernández-de-Córdova, M. Barturen, I. Fernández and S. Conejero, *Inorg. Chem.*, 2022, **61**, 20848–20859.
- 45 M. A. Esteruelas, A. M. López, E. Oñate and E. Raga, *Angew. Chem., Int. Ed.*, 2022, **61**, e202204081.
- 46 U. Schubert, *Adv. Organomet. Chem.*, 1990, **30**, 151–187.
- 47 S. K. Ignatov, N. H. Rees, B. R. Tyrrell, S. R. Dubberley, A. G. Razuvaev, P. Mountford and G. I. Nikonov, *Chem. – Eur. J.*, 2004, **10**, 4991–4999.
- 48 P. Meixner, K. Batke, A. Fischer, D. Schmitz, G. Eickerling, M. Kalter, K. Ruhland, K. Eichele, J. E. Barquera-Lozada, N. P. M. Casati, F. Montisci, P. Macchi and W. Scherer, *J. Phys. Chem. A*, 2017, **121**, 7219–7235.
- 49 S. Gründemann, H.-H. Limbach, G. Buntkowsky, S. Sabo-Etienne and B. Chaudret, *J. Phys. Chem. A*, 1999, **103**, 4752–4754.
- 50 R. H. Crabtree, *Chem. Rev.*, 2016, **116**, 8750–8769.
- 51 D. M. Heinekey, *J. Labelled Compd. Radiopharm.*, 2007, **50**, 1063–1071.
- 52 B. R. Bender, G. J. Kubas, L. H. Jones, B. I. Swanson, J. Eckert, K. B. Capps and C. D. Hoff, *J. Am. Chem. Soc.*, 1997, **119**, 9179–9190.
- 53 G. Parkin, *Acc. Chem. Res.*, 2009, **42**, 315–325.
- 54 C. Perthesis, M. Fan and W. D. Jones, *Organometallics*, 1992, **11**, 3622–3629.
- 55 C. R. Groom, I. J. Bruno, M. P. Lightfoot and S. C. Ward, *Acta Crystallogr., Sect. B*, 2016, **72**, 171–179.
- 56 Y. Tanabe and Y. Nishibayashi, in *Transition Metal–Dinitrogen Complexes*, ed. Y. Nishibayashi, Wiley-VCH, Weinheim, Germany, 2019, ch. 1, pp. 1–77.
- 57 A. D. Piascik and A. E. Ashley, in *Transition Metal–Dinitrogen Complexes*, ed. Y. Nishibayashi, Wiley-VCH, Weinheim, Germany, 2019, ch. 6, pp. 285–335.



- 58 N. Mézailles, in *Transition Metal–Dinitrogen Complexes*, ed. Y. Nishibayashi, Wiley-VCH, Weinheim, Germany, 2019, ch. 4, pp. 221–269.
- 59 E. A. Ison, in *Transition Metal–Dinitrogen Complexes*, ed. Y. Nishibayashi, Wiley-VCH, Weinheim, Germany, 2019, ch. 5, pp. 271–284.
- 60 Q. Le Dé, D. A. Valyaev and A. Simonneau, *Chem. – Eur. J.*, 2024, **30**, e202400784.
- 61 D. Sellmann, *Angew. Chem., Int. Ed. Engl.*, 1972, **11**, 534–534.
- 62 S. M. Howdle and M. Poliakoff, *J. Chem. Soc., Chem. Commun.*, 1989, 1099–1101.
- 63 J. A. Banister, P. D. Lee and M. Poliakoff, *Organometallics*, 1995, **14**, 3876–3885.
- 64 P. D. Lee, J. L. King, S. Seebald and M. Poliakoff, *Organometallics*, 1998, **17**, 524–533.
- 65 R. K. Merwin, A. C. Ontko, J. F. Houllis and D. M. Roddick, *Polyhedron*, 2004, **23**, 2873–2878.
- 66 J. A. Banister, M. W. George, S. Grubert, S. M. Howdle, M. Jobling, F. P. A. Johnson, S. L. Morrison, M. Poliakoff, U. Schubert and J. R. Westwell, *J. Organomet. Chem.*, 1994, **484**, 129–135.
- 67 S. M. Howdle, M. A. Healy and M. Poliakoff, *J. Am. Chem. Soc.*, 1990, **112**, 4804–4813.
- 68 Y. Zheng, W. Wang, J. Lin, Y. She and K. Fu, *J. Phys. Chem.*, 1992, **96**, 9821–9827.
- 69 W. T. Boese and P. C. Ford, *Organometallics*, 1994, **13**, 3525–3531.
- 70 J. B. Eastwood, L. A. Hammarback, M. T. McRobie, I. P. Clark, M. Towrie, I. J. S. Fairlamb and J. M. Lynam, *Dalton Trans.*, 2020, **49**, 5463–5470.
- 71 B. H. G. Swennenhuis, R. Poland, N. J. DeYonker, C. E. Webster, D. J. Darensbourg and A. A. Bengali, *Organometallics*, 2011, **30**, 3054–3063.
- 72 Y.-Q. Zou, S. Chakraborty, A. Nerush, D. Oren, Y. Diskin-Posner, Y. Ben-David and D. Milstein, *ACS Catal.*, 2018, **8**, 8014–8019.
- 73 W. A. King, X.-L. Luo, B. L. Scott, G. J. Kubas and K. W. Zilm, *J. Am. Chem. Soc.*, 1996, **118**, 6782–6783.
- 74 W. A. King, B. L. Scott, J. Eckert and G. J. Kubas, *Inorg. Chem.*, 1999, **38**, 1069–1084.
- 75 K. D. Welch, W. G. Dougherty, W. S. Kassel, D. L. DuBois and R. M. Bullock, *Organometallics*, 2010, **29**, 4532–4540.
- 76 P. DeShong, G. A. Slough, D. R. Sidler, P. J. Rybczynski, W. Von Philipsborn, R. W. Kunz, B. E. Bursten and T. W. Clayton Jr., *Organometallics*, 1989, **8**, 1381–1388.
- 77 J. D. Cotton and R. D. Markwell, *Inorg. Chim. Acta*, 1990, **175**, 187–191.
- 78 Z.-L. Xue and T. M. Cook, in *Comprehensive Inorganic Chemistry III*, ed. J. Reedijk and K. R. Poeppelmeier, Elsevier, Oxford, 3rd edn, 2023, pp. 660–744.
- 79 W. J. Miles Jr., B. B. Garrett and R. J. Clark, *Inorg. Chem.*, 1969, **8**, 2817.
- 80 B. Wrackmeyer, T. Hofmann and M. Herberhold, *J. Organomet. Chem.*, 1995, **486**, 255.
- 81 S. Onaka, T. Miyamoto and Y. Sasaki, *Bull. Chem. Soc. Jpn.*, 1971, **44**, 1851.
- 82 W. Levason, S. D. Orchard and G. Reid, *Organometallics*, 1999, **18**, 1275–1280.
- 83 J. Connolly, M. K. Davies and G. Reid, *J. Chem. Soc., Dalton Trans.*, 1998, 3833–3838.
- 84 J. Connolly, G. W. Goodban, G. Reid and A. M. Z. Slawin, *J. Chem. Soc., Dalton Trans.*, 1998, 2225–2232.
- 85 W. Levason, L. P. Ollivere, G. Reid, N. Tsoureas and M. Webster, *J. Organomet. Chem.*, 2009, **694**, 2299–2308.
- 86 X.-X. Zhao, J. Wei and Z. Xi, *Chin. J. Chem.*, 2023, **41**, 2400–2407.
- 87 A. H. Klahn-Oliva, R. D. Singer and D. Sutton, *J. Am. Chem. Soc.*, 1986, **108**, 3107.
- 88 J. J. Carbó, O. Eisenstein, C. L. Higgitt, A. H. Klahn, F. Maseras, B. Oelckers and R. N. Perutz, *J. Chem. Soc., Dalton Trans.*, 2001, 1452–1461.
- 89 J. A. Calladine, O. Torres, M. Anstey, G. E. Ball, R. G. Bergman, J. Curley, S. B. Duckett, M. W. George, A. I. Gilson, D. J. Lawes, R. N. Perutz, X.-Z. Sun and K. P. C. Vollhardt, *Chem. Sci.*, 2010, **1**, 622–630.
- 90 D. Sellmann, *Angew. Chem., Int. Ed. Engl.*, 1971, **10**, 919–919.
- 91 Q. Le Dé, A. Bouammali, C. Bijani, L. Vendier, I. del Rosal, D. A. Valyaev, C. Dinoi and A. Simonneau, *Angew. Chem., Int. Ed.*, 2023, **62**, e202305235.
- 92 C. Barrientos-Penna and D. Sutton, *J. Chem. Soc., Chem. Commun.*, 1980, 111–112.
- 93 F. M. Bickelhaupt and E. J. Baerends, in *Rev. Comput. Chem*, ed. D. B. Boyd and K. B. Lipkowitz, Wiley-VCH, New York, 2000, pp. 1–86.
- 94 T. Ziegler and A. Rauk, *Inorg. Chem.*, 1979, **18**, 1755–1759.
- 95 T. Ziegler and A. Rauk, *Inorg. Chem.*, 1979, **18**, 1558–1565.
- 96 S. M. N. V. T. Gorantla and K. C. Mondal, *ACS Omega*, 2021, **6**, 33932–33942.
- 97 S. M. N. V. T. Gorantla and K. C. Mondal, *ACS Omega*, 2021, **6**, 33389–33397.
- 98 K. Devi, S. M. N. V. T. Gorantla and K. C. Mondal, *Eur. J. Inorg. Chem.*, 2022, **2022**, e202100931.
- 99 S. M. N. V. T. Gorantla, H. S. Karnamkkott, S. Arumugam, S. Mondal and K. C. Mondal, *J. Comput. Chem.*, 2023, **44**, 43–60.
- 100 H. S. Karnamkkott, S. M. N. V. T. Gorantla and K. C. Mondal, *J. Chem. Sci.*, 2024, **136**, 55.
- 101 P. W. Smith and T. D. Tilley, *J. Am. Chem. Soc.*, 2018, **140**, 3880–3883.
- 102 X. Yang and C. Wang, *Angew. Chem., Int. Ed.*, 2018, **57**, 923–928.
- 103 G. M. Bancroft, H. C. Clark, R. G. Kidd, A. T. Rake and H. G. Spinney, *Inorg. Chem.*, 1973, **12**, 728.
- 104 F. Calderazzo, E. A. C. Lucken and D. F. Williams, *J. Chem. Soc. A*, 1967, 154.
- 105 M. K. Davies, M. C. Durrant, W. Levason, G. Reid and R. L. Richards, *J. Chem. Soc., Dalton Trans.*, 1999, 1077–1084.
- 106 J. Connolly, A. R. J. Genge, W. Levason, S. D. Orchard, S. J. A. Pope and G. Reid, *J. Chem. Soc., Dalton Trans.*, 1999, 2343–2352.



- 107 B. J. Burger and J. E. Bercaw, in *Experimental Organometallic Chemistry - A Practicum in Synthesis and Characterization*, American Chemical Society, Washington, D.C., 1987, vol. 357, pp. 79–98.
- 108 K. V. Zaitsev, I. P. Gloriov, Y. F. Oprunenko, E. K. Lermontova and A. V. Churakov, *J. Organomet. Chem.*, 2019, **897**, 217–227.
- 109 R. K. Harris, E. D. Becker, S. M. Cabral de Menezes, R. Goodfellow and P. Granger, *Pure Appl. Chem.*, 2001, **73**, 1795–1818.
- 110 G. M. Sheldrick, *Acta Crystallogr., Sect. A: Found. Adv.*, 2015, **71**, 3–8.
- 111 G. M. Sheldrick, *Acta Crystallogr., Sect. C: Struct. Chem.*, 2015, **71**, 3–8.
- 112 O. V. Dolomanov, L. J. Bourhis, R. J. Gildea, J. A. K. Howard and H. Puschmann, *J. Appl. Crystallogr.*, 2009, **42**, 339–341.
- 113 ADF 2020.102, SCM, Theoretical Chemistry, Vrije Universiteit, Amsterdam, The Netherlands, <https://www.scm.com>.
- 114 G. te Velde, F. M. Bickelhaupt, E. J. Baerends, C. Fonseca Guerra, S. J. A. Van Gisbergen, J. G. Snijders and T. Ziegler, *J. Comput. Chem.*, 2001, **22**, 931–967.
- 115 J. P. Perdew, K. Burke and M. Ernzerhof, *Phys. Rev. Lett.*, 1996, **77**, 3865–3868.
- 116 E. van Lenthe, E. J. Baerends and J. G. Snijders, *J. Chem. Phys.*, 1993, **99**, 4597–4610.
- 117 E. van Lenthe, E. J. Baerends and J. G. Snijders, *J. Chem. Phys.*, 1994, **101**, 9783–9792.
- 118 E. van Lenthe, A. Ehlers and E.-J. Baerends, *J. Chem. Phys.*, 1999, **110**, 8943–8953.
- 119 E. van Lenthe, J. G. Snijders and E. J. Baerends, *J. Chem. Phys.*, 1996, **105**, 6505–6516.
- 120 E. van Lenthe, R. van Leeuwen, E. J. Baerends and J. G. Snijders, *Int. J. Quantum Chem.*, 1996, **57**, 281–293.
- 121 S. Grimme, J. Antony, S. Ehrlich and H. Krieg, *J. Chem. Phys.*, 2010, **132**, 154104.
- 122 S. Grimme, S. Ehrlich and L. Goerigk, *J. Comput. Chem.*, 2011, **32**, 1456–1465.
- 123 A. D. Becke, *J. Chem. Phys.*, 1988, **88**, 2547–2553.
- 124 M. Franchini, P. H. T. Philipsen and L. Visscher, *J. Comput. Chem.*, 2013, **34**, 1819–1827.
- 125 A. Bérces, R. M. Dickson, L. Y. Fan, H. Jacobsen, D. Swerhone and T. Ziegler, *Comput. Phys. Commun.*, 1997, **100**, 247–262.
- 126 H. Jacobsen, A. Bérces, D. P. Swerhone and T. Ziegler, *Comput. Phys. Commun.*, 1997, **100**, 263–276.
- 127 S. K. Wolff, *Int. J. Quantum Chem.*, 2005, **104**, 645–659.
- 128 T. Ziegler and A. Rauk, *Inorg. Chem.*, 1979, **18**, 1755–1759.
- 129 T. Ziegler and A. Rauk, *Inorg. Chem.*, 1979, **18**, 1558–1565.
- 130 M. Mitoraj and A. Michalak, *Organometallics*, 2007, **26**, 6576–6580.
- 131 A. Michalak, M. Mitoraj and T. Ziegler, *J. Phys. Chem. A*, 2008, **112**, 1933–1939.
- 132 M. P. Mitoraj, A. Michalak and T. Ziegler, *Organometallics*, 2009, **28**, 3727–3733.
- 133 M. P. Mitoraj, A. Michalak and T. Ziegler, *J. Chem. Theory Comput.*, 2009, **5**, 962–975.
- 134 C. J. Jameson, in *eMagRes*, ed. R. K. Harris and R. L. Wasylishen, John Wiley & Sons, Ltd., 2007.
- 135 A. J. Jordan, C. M. Wyss, J. Bacsá and J. P. Sadighi, *Organometallics*, 2016, **35**, 613–616.

